

CZECH TECHNICAL UNIVERSITY IN PRAGUE

Faculty of Mechanical Engineering

Department of Material Engineering



MASTER'S THESIS

Effect of heat treatment on structure and mechanical properties of spring steel

Author: Bc. Otakar Kuchař
Study programme: Production and Material Engineering
Supervisor: Doc. Ing. Jana Sobotová, Ph.D.

Prague 2019

I. OSOBNÍ A STUDIJNÍ ÚDAJE

Příjmení: **Kuchař** Jméno: **Otakar** Osobní číslo: **437116**
Fakulta/ústav: **Fakulta strojní**
Zadávací katedra/ústav: **Ústav materiálového inženýrství**
Studijní program: **Strojní inženýrství**
Studijní obor: **Výrobní a materiálové inženýrství**

II. ÚDAJE K DIPLOMOVÉ PRÁCI

Název diplomové práce:

Vliv tepelného zpracování na vlastnosti pružinové oceli 54SiCr6

Název diplomové práce anglicky:

Effect of heat treatment on properties of 54SiCr6 spring steel

Pokyny pro vypracování:

1. Literární rešerše
2. Experimentální část
Tepelné zpracování vzorků
Hodnocení mechanických vlastností a struktury
3. Vyhodnocení a diskuse výsledků, závěry, sepsání DP

Seznam doporučené literatury:

- [1] ČSN EN ISO 6892-1. Kovové materiály - Zkouška tahem: Část 1. Zkušební metoda za pokojové teploty. Praha: Úřad pro technickou normalizaci, metrologii a zkušebnictví, 2010.
[2] PTÁČEK, L. Nauka o materiálu II. Brno: CERM, c1999. ISBN 80-720-4130-4.
[3] MACEK, K., J. JANOVEC, P. JURČI a P. ZUNA. Kovové materiály. Vyd.1. Praha: Česká technika-nakladatelství ČVUT, 2006. ISBN 80-101-3513-1.

Jméno a pracoviště vedoucí(ho) diplomové práce:


doc. Ing. Jana Sobotová, Ph.D., ústav materiálového inženýrství FS

Jméno a pracoviště druhé(ho) vedoucí(ho) nebo konzultanta(ky) diplomové práce:

Datum zadání diplomové práce: **17.10.2019**

Termín odevzdání diplomové práce: **08.01.2020**

Platnost zadání diplomové práce:


doc. Ing. Jana Sobotová, Ph.D.
podpis vedoucí(ho) práce

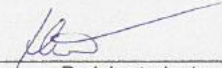

prof. RNDr. Petr Špatenka, CSc.
podpis vedoucí(ho) ústavu/katedry


prof. Ing. Michael Valášek, DrSc.
podpis děkana(ky)

III. PŘEVZETÍ ZADÁNÍ

Diplomant bere na vědomí, že je povinen vypracovat diplomovou práci samostatně, bez cizí pomoci, s výjimkou poskytnutých konzultací. Seznam použité literatury, jiných pramenů a jmen konzultantů je třeba uvést v diplomové práci.

29.10.2019
Datum převzetí zadání


Podpis studenta

Declaration

I declare, that I have elaborated this work independently and have used the literature listed in the cited sources.

In Prague: 07. 01. 2020



Signature

Acknowledgment

Thank you Mrs. doc. Ing. Jana Sobotová, Ph.D for her professional guidance and valuable comments in the elaboration of this thesis and above all for the patient approach during numerous consultations.

Furthermore, Mr. doc. Ing. Václav Machek, CSc. for valuable comments and professional advice during the work, Mrs. Ing. Elena Čižmárová, Ph.D and Mr. Ing. Jan Krčil for his support and assistance in processing mechanical tests and preparing metallographic samples.

Last but not least, I would like to thank Muhr und Bender KG, especially Mr. Ing. Daniel Snížek and Mr. Ing. Luboš Grach for performing all the tests within the company and for valuable comments during them.

ABSTRACT

The work is focused on evaluation of properties and structure of spring steel 54SiCr6 for different heat treatment conditions. Specimens A were stress relief annealed for 20 and 40 minutes at 300, 340, 380 and 420 °C in a laboratory furnace. In addition, the specimens were subjected to the tensile test, modified impact test, some of them to the Vickers hardness test and metallographic analysis. Specimens B – springs were annealed for 20 minutes at 300, 340, 390 and 410 °C in a gas continuous furnace. At the same time, the springs were measured for the winding angle before and after the heat treatment and also after the vibration bath, which followed the heat treatment process. Durability tests and X-ray diffraction analysis were performed on selected springs. The influence of the annealing temperature on the properties of the monitored states was proved, while the choice of the annealing time (20 and 40 minutes) has no significant effect. The temperature of 420 °C seems unsuitable in view of the results obtained.

Keywords: stress relief annealing, spring steel, spring wire, 54SiCr6, mechanical properties, structure, residual stress, stress, tempering

ABSTRAKT

Práce se zabývá hodnocením vlastností a struktury pružinové oceli 54SiCr6 v rámci různých podmínek tepelného zpracování. Vzorky A byly žíhány ke snížení pnutí při teplotě 300, 340, 380 a 420 °C po dobu 20 a 40 minut v laboratorní pídce. U těchto vzorků byla provedena zkouška tahem, modifikované zkouška rázem v ohybu, u části z nich zkouška tvrdosti dle Vickerse a metalografická analýza. Vzorky B – pružiny byly žíhány při teplotě 300, 340, 390 a 410 °C po dobu 20 minut v plynové průběžné peci. Zároveň bylo u pružin uskutečněno měření úhlu navinutí před a po tepelném zpracování a také po vibrační lázni. U vybraných pružin byly provedeny zkoušky životnosti, u dalších vybraných poté rentgenová difrakční analýza. Teplota žíhání má vliv na vlastnosti sledovaných stavů. Naopak rozdíl doby žíhání (20 a 40 minut) se ukázal jako nevýrazný. Teplota 420 °C se z hlediska dosažených výsledků jeví jako nevhodná.

Klíčová slova: žíhání ke snížení pnutí, pružinová ocel, pružinový drát, 54SiCr6, mechanické vlastnosti, struktura, zbytkové pnutí, napětí, popouštění

Table of Contents

List of used symbols.....	8
Introduction	11
1 Theoretical view on the solved issue	12
1.1 Springs and spring steels.....	12
1.1.1 History of springs	12
1.1.2 Basic characteristics of springs	15
1.1.3 Spring steels and their distribution	18
1.2 Springs in industrial production	23
1.2.1 Industrial production of spring wire.....	23
1.2.2 Patenting.....	25
1.2.3 Quenching and tempering	26
1.3 Springs in series production	30
1.3.1 Series production of springs.....	30
1.3.2 Stress relief annealing.....	32
2 Practical part of the solved issue.....	35
2.1 Used material.....	35
2.1.1 54SiCr6.....	35
2.1.2 Specimens A.....	36
2.1.3 Specimens B: springs	38
2.2 Heat treatment – specimens A	39
2.3 Mechanical testing methods – specimens A.....	42
2.3.1 Tensile testing.....	43
2.3.2 Tensile test evaluation methods	44
2.3.3 Modified impact test	47
2.3.4 Vickers microhardness test	48
2.4 Metallographic analysis – specimens A.....	49
2.5 Heat treatment – specimens B	50
2.5.1 Stress relief annealing, testing and measurement.....	50
2.6 X-ray diffraction – specimens B.....	53
2.6.1 Residual stresses.....	53

2.6.2	X-ray strain gauging	54
2.7	Durability test – specimens B	57
2.8	Overview of specimens, tests and measurements.....	58
3	Results and discussion.....	59
3.1	Mechanical testing methods – specimens A.....	59
3.1.1	Tensile testing	59
3.1.2	Strength and hardness parameters (R_m , $R_{p0.2}$, HV1)	62
3.1.3	Ductile characteristics ($A_{100\text{ mm}}$, Z)	65
3.1.4	Plasticity stock (PS) and toughness parameter (λ).....	67
3.2	Metallographic analysis – specimens A.....	69
3.3	Winding angle measurements – specimens B.....	71
3.4	X-ray diffraction – specimens B.....	72
3.5	Durability tests – specimens B	73
3.6	General assessment of the HT effect – 4.25 mm wire	74
	Conclusion	75
	Bibliography	76
	List of figures.....	79
	List of tables.....	80

List of used symbols

BC	Before Christ
L. da V.	Leonardo da Vinci
CAD	Computer Aided Design
2D	Two-Dimensional
3D	Three-Dimensional
4D	Four-Dimensional
LIFT	Lightweight Innovative Flexible Technology
F [N; kN]	Force
M [Nm; Nmm]	Moment (Torque)
σ [MPa = Nmm ⁻²]	Normal stress
τ [MPa = Nmm ⁻²]	Torsional stress
Si [%]	Silicium
Cr [%]	Chromium
V [%]	Vanadium
Ni [%]	Nickel
Mn [%]	Manganese
C [%]	Carbon
$R_{p0,2}$ [MPa = Nmm ⁻²]	Yield strength at permanent deformation 0,2 %
R_m [MPa = Nmm ⁻²]	Tensile strength
max.	maximum
min.	minimum
HV [-]	Vickers Hardness
HV1 [-]	Vickers Hardness – load 9.8 N (1 kg)
P [%]	Phosphorus

S [%]	Sulfur
Mo	Molybdenum
X	Medium content at least one alloying element $\geq 5\%$
Fe [%]	Iron
TTT	Time-Temperature-Transformation
IT	Isothermal Transformation
Z [%]	Reduction of area (contraction)
A [%]	Percent elongation (overall ductility)
A_g [%]	Plastic ductility
X-ray	X-radiation (electromagnetic wave)
t [min]	Time
T [°C; °F]	Temperature
τ_r [MPa = Nmm ⁻²]	Resulting torsional stress
HSLA	High-Strength Low-Alloy
Nb [%]	Niobium
Ti [%]	Titanium
Cu [%]	Copper
H [%]	Hydrogen
\varnothing [mm]	Diameter
$A_{11.3}$ [%]	Percent elongation of a gauge length (L_0) of $11.3\sqrt{S_0}$
$A_{100\text{ mm}}$ [%]	Percent elongation of a gauge length (L_0) of 100 mm
ΔL [mm]	Increment of original measured length
L_0 [mm]	Original measured length
ΔA [mm ²]	Differ. between orig. and broken cross-section area
A_0 [mm ²]	Original cross-section area
PS [MPa = Nmm ⁻² = 10^{-3} Jmm ⁻³]	Plasticity stock

ε_g [-]	Permanent engineering strain
P220	Granularity
P1200	Granularity
μm	Unit - micrometer
O	Oxygen
O ₂	Oxygen in molecular form
SiO ₂	Silicon dioxide
ε [-]	Engineering strain (ratio elongation)
R [MPa = Nmm ⁻²]	Engineering stress
f [Hz]	Frequency
σ_{ij} [MPa = Nmm ⁻²]	Stress tensor components
T [mm]	Distance from the surface
$CrK\alpha$	X-ray tube with chrome anode; X-ray beam
A_m [mm]	Arithmetic mean
s [-]	Corrected standard deviation

Introduction

Spring manufacturers are currently looking for a way to meet the ever-increasing performance requirements of their products. High demands are placed on quality, non-scrap rates and production efficiency. One of many manufacturers is Muhr und Bender KG (Mubea). The company is a global automotive supplier and innovative specialist in lightweight construction. Mubea also manufactures springs for various applications in the automotive industry. Belt tensioners for combustion engines are one application. The tensioners serve as belt tensioning of the motor unit, vibration damping and also prevent belt slippage [1], [2], [3].

The increasing use of springs also requires a greater range of properties. Generally, the materials from which the springs are made are subject to high demands. Above all, it must have high strength and at the same time it must allow large elastic deformations. These products are used in various environments in which they must not lose their properties [1], [3]. A wide range of metallic and non-metallic materials are used for spring production. Recent trends include the increasingly widespread use of composite materials that can be used for spring production even for the most demanding applications at higher temperatures. Yet, the most commonly used category of spring materials are steels, especially low-alloy high strength steels [1], [4].

Heat treatment is currently an indispensable element of production. The aim of heat treatment is to achieve the required mechanical, technological and other characteristics of a product or semi-finished product. An integral part of the production of springs is their heat treatment in the form of stress relief annealing. This heat treatment is included in the production after the cold forming of the spring wire, since in this process large plastic and elastic deformations occur in the wire cross-section leading to residual stresses.

The aim of the Master's thesis is research and evaluation of heat treatment parameters and influence of this process on the properties of springs made of low-alloy high strength steel 54SiCr6. The research was partly carried out at the Department of Material Engineering, CTU in Prague and also at Mubea. The work was developed based on the requirements of this company, where 54SiCr6 steel is used for spring production.

1 Theoretical view on the solved issue

In the first part of my thesis is included the theory, that deals with the issue. This chapter summarizes the information about springs and spring wires, the materials used to make them, also their production, their mechanical stresses and primarily the heat treatment of these products.

1.1 Springs and spring steels

1.1.1 History of springs

It is well known, that springs are a symbol of high elasticity throughout their history. No less important is the ability to store potential energy. Since ancient times, people could use the properties of these technical elements and in the Stone Age, they could find the usability of a flexible wooden arch. The development from technical spring from natural material to today's steel spring is very extensive [2].

Metal spring material was first used in the Bronze Age, when dress pins began to appear around 1400 BC (Figure 1). These pins, which have been provided with up to four threads, could now be considered the ancestor of today's torsion springs. The first flat and leaf springs were also known around 250 BC. Spiral springs appeared in small padlocks around 1400 and were then known in watches since 1429 [2].



Figure 1: Dress pins from the Bronze Age (simple - 1 and threaded - 2) [5]

Since 1400, along with the development of wire drawing, the production of low carbon steel springs has been possible. Leonardo da Vinci (L. da V.) then designed a rifle lock in 1500 (Figure 2). This rifle lock was provided with a helical spring made of round wire. In 1703, springs were produced to suspend the wagons. In 1878, coil springs for engines were developed in Vienna and also in Paris [2].

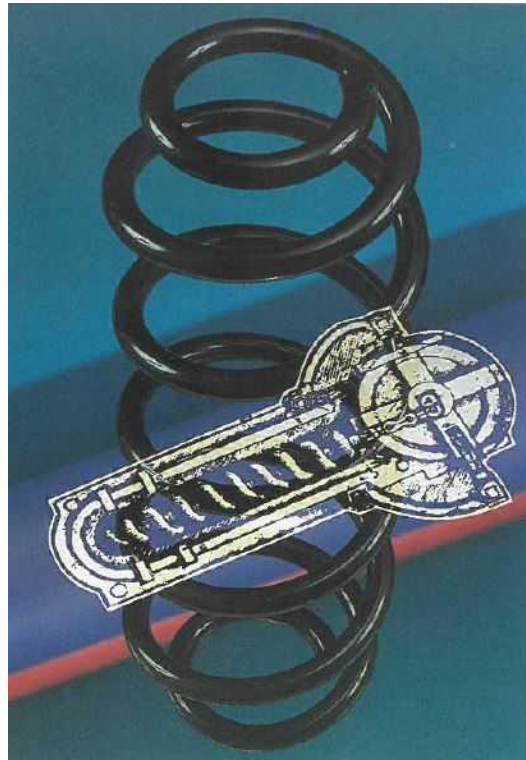


Figure 2: Rifle spring in Radschloss by L. da V. and a modern axle spring [2]

Already in 1804 in London, a certain Obadiah Elliot had a patent for the first vehicle with metal leaf springs. In 1898, the French cyclist JM Truffault used the first type of shock absorber on his racing bike. On the fork he combined metal springs and a shock absorber based on the friction principle. A year later, American car enthusiast Edward V. Hartford saw Truffault and his bicycle in action at the Versailles race and immediately recognized the potential of that car suspension system. They both teamed up and soon provided one of the Oldsmobile cars with the shock absorbers [6].

The rise of industrial series production of coil springs was evident at the beginning of the 20th century, when in 1900 the winding machines were developed and 10 years later also fully automatic winding machines [2].

In the 20th century, the development of springs was highly dependent on the growth of the automotive industry. Increasing pressure was placed on both suppliers and manufacturers themselves. This resulted in relatively rapid and constant development of new types of springs as well as their materials. Steel springs thus met the most demanding requirements in terms of drive, chassis and, last but not least, the car body [2].

However, what is common in most of today's vehicles are coil springs, which found their place on the chassis of cars in 1906 thanks to William Brush. Two years before, William was driving his brother's Crestmobile and crashed on an unpaved road. Crestmobile had only suspension using leaf springs, and on bumps, Brush lost control of the car due to wheel vibrations, slipped into a ditch and overturned. Just a few hours after the incident, Brush started to work on the car as he imagined [6].

In two years he built the type Runabout, which was equipped with the already mentioned coil springs. In addition to these, Brush installed shock absorbers on the axles of the car, giving birth to the first car with a combination of springs and shock absorbers. It is interesting that the shock absorbers on Runabout came from the already mentioned company of Edward V. Hartford [6].

At present, the development of springs is greatly supported by various CAD software products, which makes it possible to design springs of very large but also very small dimensions. They can be springs that can hold buildings throughout the earthquake. On the other hand, there are 30 micrometer variations for medical use or miniature coils used in phones, touchpads and other electrical devices. Thus, CAD software products allow us to produce springs in a variety of sizes, shapes and properties with great precision. Furthermore, technologies such as 2D materials, 3D printing and even 4D printing are beginning to appear. Even in these technologies we could find considerable potential for the future development of springs and spring materials. *The Massachusetts Institute of Technology* is currently trying to use 4D printing to create objects that can be transformed in different ways or assembled by themselves. The 2D material technology represents very weak material layers in the size of several atoms. For example, 2D graphene material, respectively a crystalline allotropic modification of carbon, is in terms of weight several times stronger than most steels. Also, the elongation capability of up to 480 % with a stable coefficient of elasticity at 100,000 stretch was found in graphene [7].

An innovation in the automotive industry is the revolutionary LIFT suspension system (Lightweight Innovative Flexible Technology) without the use of conventional springs and shock absorbers, on which the British company Ariel, industrial company Warwick

and also computer engineers from Simpack cooperated. This system is up to 40 % lighter in comparison to traditional systems, improves driving performance and overall vehicle dynamics, and last but not least, generates electricity. It is made up of a pair of hinged arms that are made of composite fibers assembled in a very precise scheme. This fiber composition allows not only suspension, but also dampening of the entire car system (Figure 3) [8].

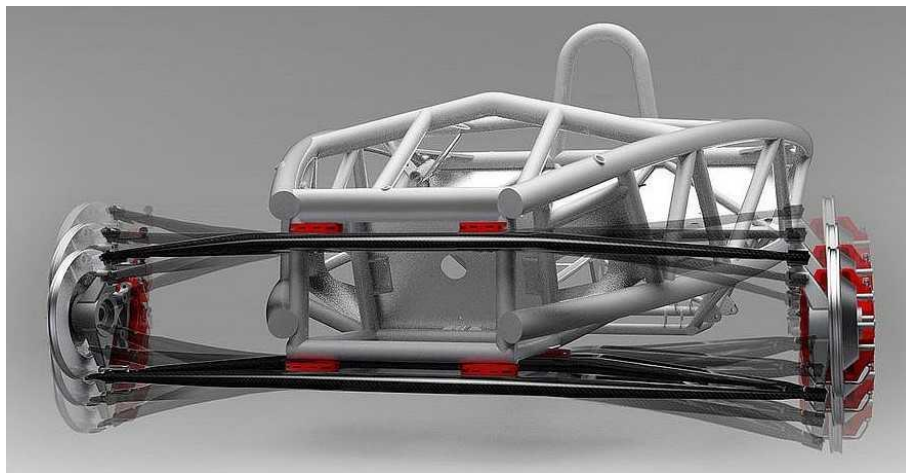


Figure 3: LIFT suspension system by Ariel [8]

1.1.2 Basic characteristics of springs

Springs have the ability to store and deliver mechanical work. They also have the property of absorbing hard impacts. They are maintenance-free and their production speed is relatively high [2]. For example, an internal source of company Mubea states, that the production line can produce up to 2,000 springs per hour.

Their use is very diverse [2]:

- They move the respective parts in predefined direction and further in the opposite direction until they reach the original position. This includes, for example, valve springs used in automotive combustion engines, also return springs in brakes, brake fans, clutches and also in measuring instruments.
- Shock and vibration damping on passenger car axles.

- They distribute forces and balance them. They are used in clamping tools, in upholstery, also for car body stabilization.
- They facilitate opening, keeping open and closing the bonnet or boot lid.
- They adjust the exact forces and moments, for example, to create the necessary contact forces in the vibration dampers.
- They measure and regulate forces and moments in, for example, dynamometers, such as springs directing forces in electrical measuring tools and torque dials.

Springs can be divided according to physical principle into [9], [10]:

- Mechanical,
 - o Metallic,
 - o Non-metallic,
- Pneumatic or hydro-pneumatic.

Depending on the type of stress, the springs can be divided into [9], [10]:


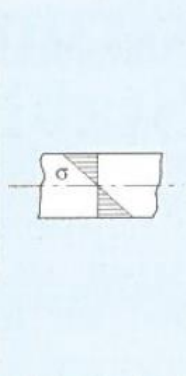

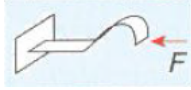


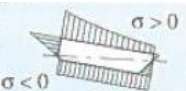

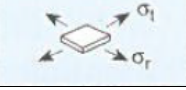



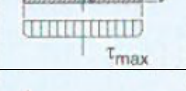

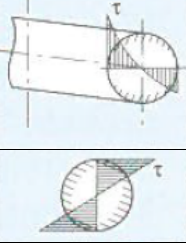

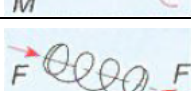

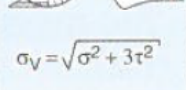

- Springs stressed by bending,
 - o Springs and spring bundles,
 - o Helical torsion springs,
 - o Spiral springs,
- Springs stressed by torsion,
 - o Helical compression or tension springs,
 - o Helical conical springs,
 - o Torsion bars,
- Springs stressed in combination,
 - o Disc springs,
 - o Ring springs (Figure 4).



Figure 4: Ring springs [11]

Many of their functions are reflected in the large number of spring shapes. The most important of the basic types classified also by their type of stress are listed in Table 1.

Table 1: Steel springs and distribution of acting forces and their stresses [2], [10]

Spring type	Distr. of forces and torques	Stress distribution	Use in	Mubea product	Stress type
Leaf spring			Utility machines – shock absorbers	Yes	Normal Stress
Spiral spring			Tensioners, Seatbelts	Yes	
Flat spring			HOLDERS, clamps, clips	Yes	
Torsion spring			Valves, clutches, gear shifters	Yes	
Disc spring			Valves, latches, couplings	Yes	
Diaphragm spring			Car clutches	Yes	
Ring spring			Pre-load and retain bearings	Yes	
Torsion leaf spring			HOLDERS, clamps, clips	No	
Compression spring			Belt tensioners	Yes	
Tension spring			Belt tensioners	Yes	
Torsion-bar spring			Belt tensioners	Yes	
Screw spring with higher pitch			Shock absorbers	Yes	Normal and tangential stress
Spatial shaped spring			$\sigma_V = \sqrt{\sigma^2 + 3\tau^2}$	HOLDERS, clamps, clips	

1.1.3 Spring steels and their distribution

Steel springs are usually made of round, flat or tubular profiles. This shape is obtained by hot or cold forming. After cold forming, there is usually a process to reduce residual stresses, such as annealing (stress relief annealing) [1].

Taking into account the production of springs from round profiles - wires, these wires are before shaping them into the desired spring form produced as follows. They are made by cold forming or hot forming. As a rule, the cold-formed round wires are made in the following ways outside the forming process itself. The patenting process is common, then quenching process using oil bath is common too [2].

Over and above, hard drawn wires or high-alloy steel wires are also used for the production of springs. Refractory, for example stainless steels, are also used if desired [1].

The properties of the materials vary and reach the desired values depending, inter alia, on the carbon content and the proportion of alloying elements such as chromium (Cr), silicon (Si) or manganese (Mn) [1].

Another source states that carbon steels are used for low stress springs. For steel wires of smaller diameters and flat wires of smaller width, the strength using cold forming can be increased. For this type of treatment, patenting or controlled cooling of the wire or belt seems to be the most suitable. The carbon content of the steel is further selected according to the strength requirements. The quenching and subsequent tempering process is then used for more stressed carbon steel products [9].

Steels (for springs) alloyed with manganese (Mn), silicon (Si), manganese and silicon, manganese and chromium (Cr), silicon and chromium (Cr), chromium and vanadium (V) are referred to as low alloy. For the most stressed springs, steels are alloyed with chromium, nickel (Ni), molybdenum (Mo) and vanadium. Quenching and tempering are then an integral part of the production of these spring steels. Increased silicon content is used for better strength characteristics. The manganese content then increases the hardenability. In order to improve the resistance to tempering, chromium or vanadium is added to the material. The enriched material is then capable of withstanding operating temperatures of up to 300 °C. Hardenable chrome stainless steel finds its application in corrosive environment [9].

Decarburization, primarily with a silicon content above 1 %, may occur when steels are hot-rolled. The decarburization depth is corrected by standard or technical conditions.

According to this source and the above-mentioned information, spring steels are divided into quenched steels, patented wire steels and steels from cold-rolled strips [9].

Also according to EN 10132, cold rolled strips for spring steels are defined. Steels in soft annealed or thermal refined (quenched and tempered) state are in EN 10132 given too. All these three states of spring steel are characterized as soothed. Furthermore, the non-metallic inclusions test and the grain size test is determined. The decarburization depth reaches a maximum of 0.3 % for grades with silicon (Si) and 0.2 % for the remaining grades. The decarburization depth is measured 5 mm from the sheet edge [12], [13].

The steels are divided according to their chemical composition into [12], [13]:

- noble non-alloy steels, resp. noble carbon steels,
- alloyed silicon steels, resp. low-alloy steels,
- alloyed steels with chromium (Cr), optionally with chromium (Cr) and vanadium (V) or nickel (Ni), resp. high-alloy steels.

A characteristic of spring materials or springs is the so-called alternating and cyclic loading, whereby the spring moves from one position to another depending on the direction of force or its torque. For this reason, high demands are placed on materials for their elastic strength, yield strength, tensile strength and fatigue at alternating or combined stress. Elastic deformation is necessary because of the dynamic loading of these products and a plastic deformation due to the winding of the wire during manufacture. The toughness of the material is an integral part of the characteristic [2], [12].

The following Table 2 lists some spring steel representatives with their chemical composition.

Table 2: Spring steel representatives [12], [13]

Designation	Chemical composition					Literature
	EN	C [%]	Si [%]	Mn [%]	Cr [%]	
C40	0.37 – 0.45	0.17 – 0.37	0.50 – 0.80	max. 0.25	max. 0.30	[12]
C55S	0.52 – 0.60	0.15 – 0.35	0.60 – 0.90	max. 0,40	max. 0.30	[13]
2C60	0.57 – 0.65	0.17 – 0.35	0.50 – 0.80	max. 0.25	max. 0.30	[12]
1CS67	0.60 – 0.70	max 0.35	0.60 - 0,80	-	-	[12]
2CS85	0.80 – 0.90	0.10 – 0.30	0.20 – 0.45	-	-	[12]
70Mn4	0.70 – 0.80	0.15 – 0.35	0.90 – 1.20	max. 0,30	max. 0.40	[12]
45Si7	0.42 – 0.52	1.50 – 1.90	0.50 – 0.80	max. 0.30	max. 0.40	[12]
60Si7	0.52 – 0.68	1.50 – 1.90	0.65 – 0.90	max. 0.30	max. 0.40	[12]
102Cr6	0.95 – 1.10	0.15 – 0.35	0.20 – 0.35	1,35 - 1,60	-	[13]
54SiCr6	0.50 – 0.60	1.30 – 1.60	0.50 – 0.80	0.50 – 0.70	max. 0.50	[12]
51CrV4	0.47 – 0.55	0.17 – 0.37	0.70 – 1.00	0.90 – 1.20	-	[12]
X30Cr13	0.26 – 0.35	max. 0.70	max. 0.80	12.0 – 14.0	-	[12]
X40Cr14	0.36 – 0.45	max. 0.70	max. 0.90	12.0 – 14.0	-	[12]
C125S	1.20 – 1.30	0.15 – 0.35	0.30 – 0.60	max. 0,40	-	[13]
80CrV2	0.75 – 0.85	0.15 – 0.35	0.30 – 0.50	0,40 - 0,60	-	[13]

It is clear from the table, that the nickel (Ni) content does not exceed 0.40 %. The exception is the 54SiCr6 grade steel, where the nickel content is 0.5 %. For all steels, the sulfur (S) content is 0.025 % and phosphorus (P) 0.025 %. The molybdenum (Mo) content does not exceed 0.10 %. For 75Ni8 steel, which is not listed in the table, the exceptionally high nickel (Ni) content is 1.08 to 2.10 %. For example, the designation 80CrV2 shows the vanadium (V) content of about 0.2 %. The rapid difference in the chemical composition of each steel is in the carbon (C) content [12], [13].

Non-alloy steels are iron-carbon alloys, where the content of associated elements is not higher than defined limits (up to 2 % alloying elements). These are alloys that are capable of full austenitization, when heated. According to the metastable phase diagram iron-carbon, several types of microstructures are distinguished (Figure 5). Hypoeutectoid steels have a ferritic-pearlitic structure, eutectoid then purely pearlitic. The eutectoid microstructure is characterized by a carbon content of 0.8 %. Furthermore, a group of hypereutectoid steels can be defined, where the carbon content is above 0.8 %, but also does not exceed 2 %. From a practical point of view, hypoeutectoid steels could be characterized as structural steels and hypereutectoid as tool steels. For non-alloy steels, the standard ČSN EN 10132 specifies maximum strength characteristics in the range of 1,100 to 1,200 Nmm². The maximum hardness is then in the range of 305 to 325 HV [12], [14], [15].

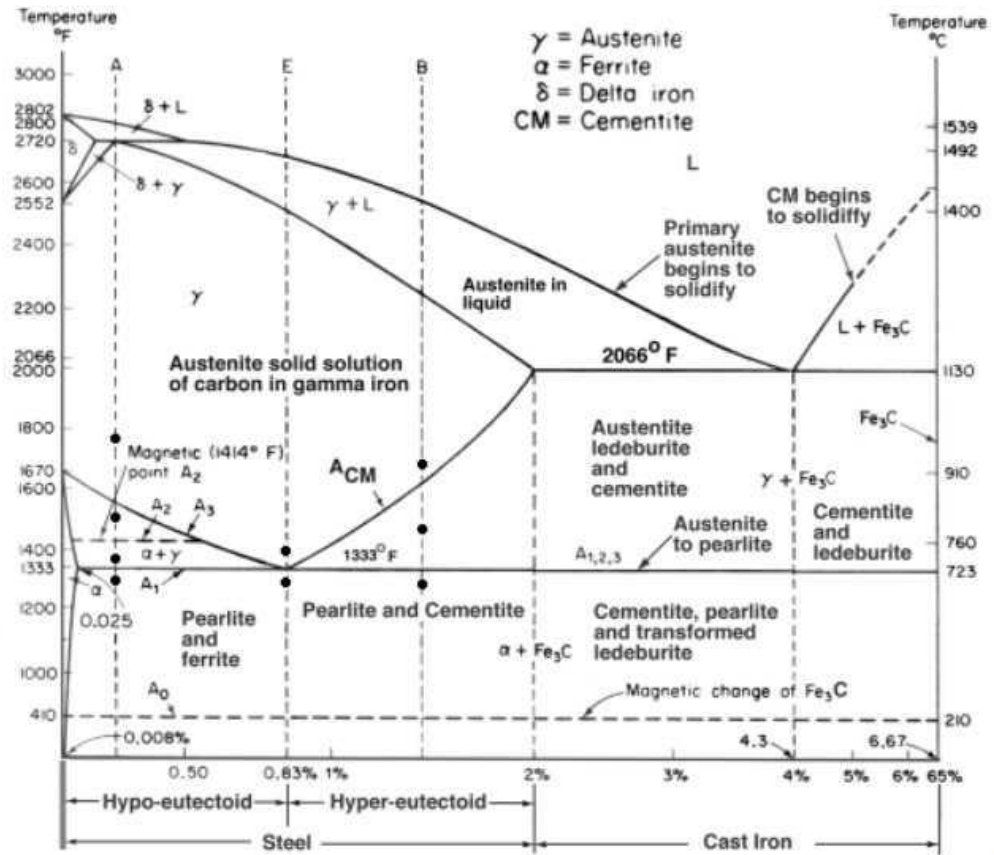


Figure 5: Phase diagram Fe-Fe₃C [16]

1.2 Springs in industrial production

1.2.1 Industrial production of spring wire

In the following, in terms of this work, only some important facts about spring production will be described.

First, the chemical composition of the spring steel is determined. After determining the chemical composition, the starting material is melted in an oxygen blowing furnace or in an electric arc furnace (Figure 6). In particular, when selecting raw materials, account must be taken of the requirement for proportions of accompanying elements. During tapping, the charge is deoxidized with aluminum or ferro-silicon, which deoxidizes, providing a better degree of purity. The subsequent metallurgical treatment consists mainly in desulphurisation steps, precise temperature setting in the ladle furnace and final treatment - gas purification, which serves to melt homogenization and separation of inclusions [4].



Figure 6: Electric arc furnace [17]

Another source states that alloying elements have a decisive influence on material properties. The resulting toughness must be so great, that the high strength spring wire can subsequently be reshaped at room temperature. Because the increase in strength is basically associated with increased notch sensitivity, non-metallic inclusions in the wire

and grooves on the wire surface of high-strength spring steels result in reduced formability, fatigue strength and overall durability leading to undesirable cracking of the material. Inclusions are ceramic nature and are not bonded to a metal matrix. The notch effect of inclusions can lead to cracking [1].

For this reason, in addition to increasing strength, efforts are being made to increase the degree of purity of the spring steel and to improve the surface quality of the rolled, hardened and tempered or patented wire [1].

Then, in the metallurgy, melt casting occurs in a continuous casting process. Finally, the aforementioned rolling operation is carried out and the result of this process is a semi - finished product known as a billet (Figure 7) [1].



Figure 7: Steel billets [18]

Springs with small or medium cross-sections are produced by cold forming and springs with larger cross-sections by hot forming. Subsequently, heat treatments and surface treatments (see the following subchapters) are carried out as well as special plasticization processes leading to a perfect wire and spring. These can then influence the spring functionality decisively. The final forming of the base body of the metal springs (see subchapter 1.3.1) takes place exclusively without the cutting process. Cutting takes place only when processing spring ends or their edges [3].

1.2.2 Patenting

Patenting of steels is a technological process that falls into the category of heat treatment. It is basically a special form of isothermal annealing. This process is characterized by holding at a temperature just above the nose temperature of the IT curve of a particular steel (Figure 8). The steel thus treated then achieves advantageous mechanical properties, which include high strength and relatively high ductility. Maintaining ductility allows further cold forming to increase of yield strength and tensile strength [19].

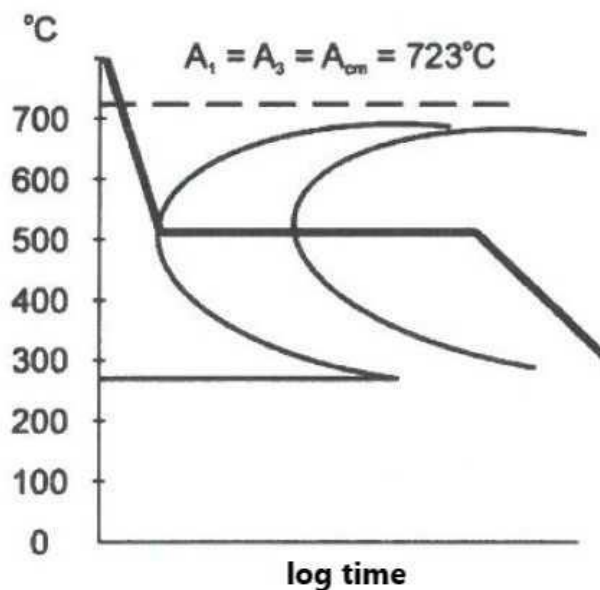


Figure 8: Patenting of unalloyed eutectoid steel in the TTT diagram (IT) [19]

The aim of patenting is to achieve the finest lamellar perlite structure. This structure is not as fragile as bainitic structure. It thus achieves higher plasticity compared to bainite. The fineness of the lamellas of the pearlitic structure is so high that it can no longer be recognized by the light microscope. An electron microscope is used to confirm this specific structure [19].

The issue presented in this chapter confirms, and also extends another source, which considers the isothermal conversion of supercooled austenite at 450 to 550 °C as the essence of patenting. The material must be heated to a temperature above the critical point before conversion (isothermal conversion) occurs. This temperature is in the range of 870 to 920 °C, which corresponds to a value of 150 to 200 °C

above the critical point. The temperature of the austenite region, the given steel gets by induction or resistance heating. This process achieves uniformity of austenite and the subsequent desired isothermal disintegration of supercooled austenite. Molten salt or molten lead is used as a subcooling bath. In the subcooling bath austenite disintegrates rapidly and a thin lamellar structure is formed. This structure is referred to as a patented sorbitol, and is a quasi-eutectoid mixture. Also the holding at the temperature takes place in metal or salt baths. [20].

This form of heat treatment is most commonly used to produce strips or wires of smaller diameter used for strings, springs or ropes. These strips or wires are made of pearlitic carbon steel. As already mentioned, these steels can be (not necessary) further cold formed, with a material removal of up to 60 % for strips and 80 % for wires [19].

What is of great importance in drawing is the size and shape of the carbides. On the one hand, the form of cementite can be defined as a thin lamellar and uniform structure, on the other hand, it is a form of cementite from mesh round pearlitic grains. In any case, the first mentioned method seems to be the most suitable for this technology. Already at the beginning of the drawing itself, there may be cracks or fragments that are revealed by the shell-type or reticular cementite. These defects can lead to rupture of the material itself. In terms of the influence of pearlite carbides in coarse lamellar form on wire ductility, they occupy an intermediary position [20].

1.2.3 Quenching and tempering

From the point of view of **quenching** not only steel products, hardenability is of major importance. The hardenability could be defined as the ability to harden the product over its entire cross-section. By quenching the material, a martensitic structure is obtained which has a substantially higher hardness than the original structure. In most cases, a volume of at least 50% martensite in the core of the product is supervised. At the end of the process, the percentage of martensite is verified according to the hardness achieved. In addition to the martensite content, the resulting hardness also depends on the percentage of carbon in the material (Figure 9) [21], [22].

The hardenability itself can be determined by Jomini's hardenability test according to EN 642. First, the Figure 9 is used, from which the corresponding value of the hardness of the layer with desired (50 %) volume of martensite for a given carbon content in the steel is taken, and then the depth of hardening is determined according to Figure 10 [21], [23].

Figure 10 represents the hardenability band of 54SiCr6 steel. 54SiCr6 is further examined in subchapter 2.1.1. The chemical composition of this steel is listed in Table 2.

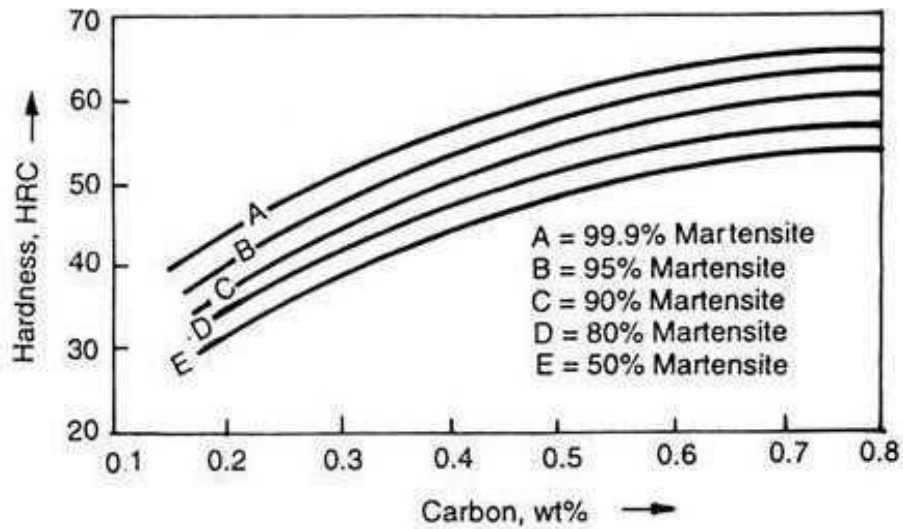


Figure 9: Relationship between C content, hardness and the amount of martensite [22]

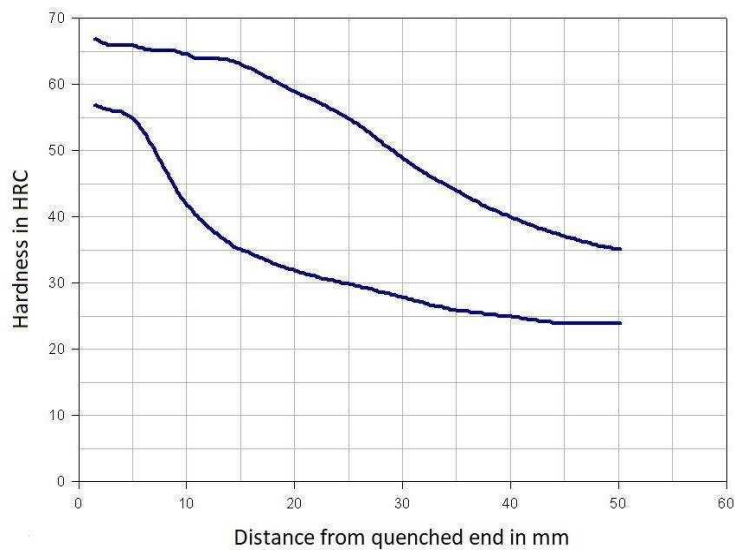


Figure 10: Hardenability diagram of 54SiCr6 steel [24]

After the volumetric quenching process, a tempering process usually occurs because of the desired product parameter settings. The main aim is to find the optimal ratio of strength and toughness of the material. In general, this process reduces hardness

and strength properties at the expense of plasticity and toughness growth. Tempering at low temperatures and tempering at high temperatures are differentiated. The difference between these temperatures is approximately 350 °C. Cemented components, cold-formed tool steels, rolling bearing steels and special steels for thermo-mechanical processing belong to the low temperature tempering group. The second group could include high-speed steels, tool steels tempered to a second hardness or structural steels. Tempering of spring steels and steels for similar applications falls within the two groups mentioned above. Therefore, the aforementioned spring steel 54SiCr6 is also included. This process also leads to significant changes in the microstructure of the material. The phase transformations concern not only the basic phases (martensite and residual austenite) but also the minor phases (carbides, carbonitrides, etc.). These phases already appear in a quenched state or arise during tempering. Minor phases are the cause of precipitation hardening to compensate for softening. This softening is caused by the transformation of martensite. The influence of temperature and tempering time of chromium steels on their hardness is shown in Figure 11 [3], [21].

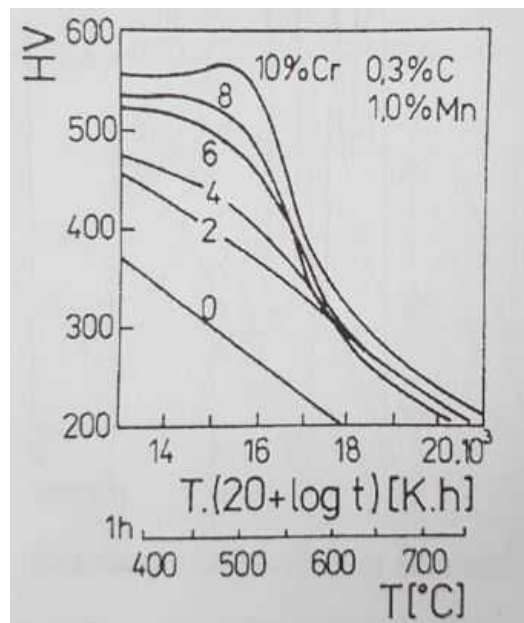


Figure 11: Chromium steels and their hardness [21]

This issue is confirmed and extended by the source according to which the true purpose of quenching and tempering of spring wires is to achieve the necessary strength properties for their function. The spring wires are usually made of normalized steels.

If 54SiCr6 steel has a tensile strength of approximately $R_m = 800 \text{ N/mm}^2$ in the annealed state, $R_m = 1450 - 2050 \text{ N/mm}^2$ can be achieved according to EN 10270-2 by quenching and tempering. The yield strength is at least $R_{p0,2} = 1300 \text{ N/mm}^2$, fracture extension at least $A_{5,65} = 6 \%$, reduction of area at least $Z = 40 \%$. The minimum values of oil hardening temperatures for this steel are $840 \text{ }^\circ\text{C}$ and the air tempering temperatures are $375 - 500 \text{ }^\circ\text{C}$ [3], [25].

The spring stiffness as a ratio of spring force to movement is dependent, for example, on the shape of the spring or its dimensions. Since these shape properties change only slightly by quenching and tempering, the spring stiffness is largely independent of heat treatment and quenching with tempering is only responsible for the load-bearing capacity of the spring. Therefore, the requirements for repetition of the heat treatment, when the spring stiffness is not reached, are generally unjustified [3], [22].

The choice of material for quenched steel wires depends on many factors such as hardenability, suitability for fine grain, decarburization tendencies, tempering resistance, etc. In principle, all steels with a carbon content $> 0.4 \%$ can be quenched. However, it should be noted that not all quenching processes are suitable for every steel [22].

Conventional quenching agents, such as hardening oil, are often used in conventional quenching for many shape solutions, especially flat and leaf. For more complicated shapes that tend to change, rapid heating in a hot bath is possible [3].

Bainitization, an isothermal structural conversion to bainite (also known as isothermal refining), is a heat treatment that leads to small changes in shapes and dimensions. In addition to this property, this heat treatment is suitable, due to the resulting fine structure, especially for oscillation loaded springs. However, it is less suitable for highly statically loaded springs because isothermally refined steels have a much lower yield strength than conventional heat treated steels. For thin cross - sections of carbon spring steels, bainitization is also feasible. Alloyed spring steels such as 51CrV4 or 61SiCr7 are suitable for thicker cross-sections [3].

The highest strength properties can be achieved by austenitic quenching. It is a thermo-mechanical treatment in which the transformation and temperature are controlled over time so that no significant recrystallization of austenite occurs [3].

To avoid damaging the spring function, it is always necessary to ensure uniform and stable heating during the heat treatment. As a result, stresses can be avoided, the risk

of cracking can be reduced and overheating with grain coarsening as well as decarburization can be avoided [3], [22].

1.3 Springs in series production

1.3.1 Series production of springs

At the end of the entire industrial production process, the spring wire is usually wrapped in coils and then exported. Mubea Company has several suppliers of these coils. The supplied spring wire is subsequently processed by the company. The result of the entire process is the final product in the form of a spring. In the next few chapters, the production process of springs is briefly mentioned, from the initial phase of unwinding the wire from the coil to the final adjustment of the spring itself, based on the knowledge gained in this company. The main attention is paid to the stress relief annealing process in subchapter 1.3.2 that is of fundamental importance from the point of view of investigation in this work.

First, the differently profiled or more often round profiled wire from the coil placed on the winch is straightened by means of feed rollers and guide elements located in a two - level straightening equipment. The equipment is a part of the spring winding machine, where the wire is gradually fed (Figure 12). The wire is then bent to the desired shape using winding tools. Once the desired geometry is achieved, the separating blade cuts the spring body from the wire.



Figure 12: Spring winding machine Wafios FMU 6.7

The spring is then moved by means of a conveyor belt into a continuous gas dual-zone furnace (Figure 13). In this furnace, the residual stresses generated by the previous winding process are reduced by annealing. More about this process is in the following subchapter.



Figure 13: Continuous gas dual-zone furnace Ipsen

After the heat treatment, the springs are transferred to an abrasive shot peening machine where the springs are surface treated. This surface shot peening treatment, according to Mubea's internal source, with steel balls with a diameter of 0.4 - 0.8 mm and a hardness of approximately 640 HV takes 10 to 12 minutes. In this process, the steel granulate pushes the surface layer of the spring and leaves small domes on it. This results in the elimination of undesirable tensile stresses in the cross-section of the material.

Shot peening of the spring is followed by 100 % inspection in the form of output tests. As a rule, the inner diameter of the spring, the height of the spring, the spacing between the coils or the winding angle itself are measured.

If necessary, the springs are subjected to a lacquer finish at the end of production.

1.3.2 Stress relief annealing

As already mentioned, after winding the wire into the desired spring shape, the stress relief annealing process occurs. It is a kind of annealing without recrystallization, when minimal changes of mechanical properties and material microstructure are required. In order to prevent the formation of cracks, in our case after the cold winding of the spring wire, it is necessary to reduce residual stresses caused by this process. An important factor is the choice of annealing temperature. This depends primarily on the type of material used. For structural steels, the temperature is usually chosen in the range of 450 to 650 °C. For cast irons this temperature does not exceed 550 °C and for low alloy weldable steels with an increased yield strength the temperatures are in the range of 530 to 580 °C. With these steels, precipitation hardening occurs as the temperature rises. These values are distant from the surface hardened parts which are annealed at temperatures of 150 to 200 °C, as they risk a significant reduction in hardness. Therefore, the most appropriate ratio is chosen to reduce residual stresses as much as possible while maintaining acceptable hardness [21]. For springs made of 54SiCr6 steel and steels of similar properties, temperatures in the range of 300 to 380 °C are selected [26]. The choice of these temperatures depends on a specific manufacturing company, on the particular setting. The specific selection of these temperatures according to Mubea Company is then described below.

The springs, respectively wires of 54SiCr6 are from previous industrial production inductively hardened and tempered. When selecting the temperatures of stress relief annealing, the lower limit is determined in dependence on the yield strength reduction necessary to reduce the stresses by plastic deformation. The upper temperature limit is primarily influenced by the tempering temperature of the thermal refined (quenched and tempered) steels, as tempering could lead to the impending decline in strength characteristics. However, the limit should be above the operating temperature of the product too [3].

According to a conventional source, the heating rate and cooling rate in the furnace during the annealing should be low. Slow heating results in uniform heating throughout the material cross-section. Therefore, the products should be placed in a cold furnace with air circulation. Slow heating, as already mentioned, reduces the yield strength. Equally important is the last part of stress relief annealing process, namely cooling

from the annealing temperature. Here, ultimately, the volume of residual stresses in the product is decided. The cooling rate should generally be from 50 to 100 °C/h [21].

A more recent study points to the use of electrically assisted annealing to reduce residual stresses in springs used in the automotive industry. This primarily involves reducing the time required for the entire process by utilizing the effect of electroplasticity and increased temperature. The experiment was performed on a sample made of spring of POSHIS 125 material similar composition to the material 54SiCr6. The spring was made of cold-coiled wire, as is common in springs intended for the automotive industry. At the beginning of the process, the sample was heated to a temperature of 380 °C within a few seconds. The sample was then held at a given constant temperature using a periodically applied, pulsed electric current, which took approximately 20 minutes from the beginning of the process. Subsequently, the power was turned off and the sample was slowly cooled down to ambient temperature (Figure 14) [26].

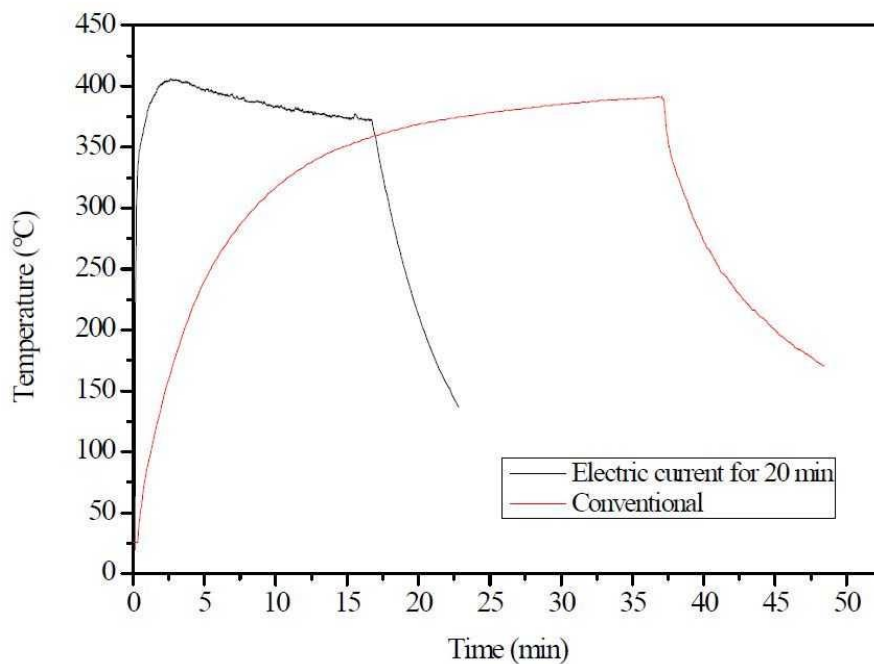


Figure 14: Stress relief annealing types comparison (t-T) [26]

The results show that the performance of electrically assisted annealing considerably exceeds conventional stress relief annealing technology when time and also energy is reduced. X-ray diffraction also points to a rapid improvement in dislocation

removal results (Figure 15). As shown in the figure, the tensile stress was removed after 1 minute during the experiment. By holding at the annealing temperature, the tensile stress was transformed into a compressive stress that is desirable for the durability of the material. Also the compressive stress was changed, not transformed, but only reduced, so its type remained unchanged [26].

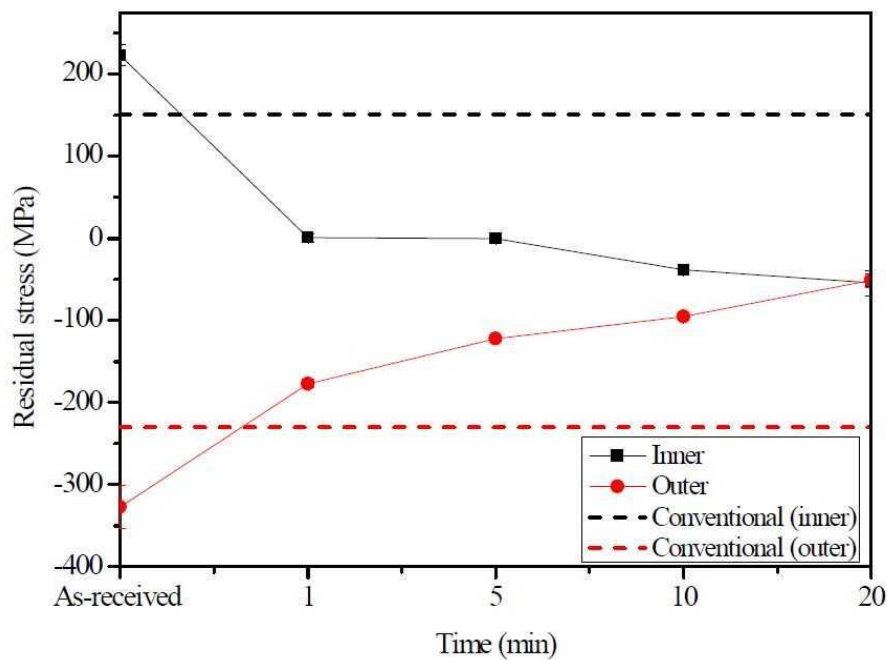


Figure 15: Stress relief annealing types comparison – t -Residual stress [26]

When the wire is cold-coiled into desired spring shape, plastic deformation of the material occurs, resulting in residual stresses in the wire cross-section. These residual stresses represent the difference between the load and the subsequent elastic suspension. Basically, after winding the wire, tensile stress appear along the inner circumference of the wire. On the other hand, there is compressive stress along the outer circumference. It is clear from these statements above that the stress generated along the inner circumference significantly reduce the product life, and that is why the stress relief annealing process is so important. More about deformation-stress issue is in chapter 2.6.1.

2 Practical part of the solved issue

2.1 Used material

2.1.1 54SiCr6

It is a high-strength low-alloy steel. In general, high-strength low-alloy (HSLA) steels are known for their good mechanical properties due to specific alloying elements in combination with a targeted microstructure. The microstructure is usually two-phase or fully martensitic form production and selected heat treatment. Hardening and tempering is very common. The alloying elements are most often Mn, Si, Cr, Mo, niobium (Nb), V or titanium (Ti) [27].

The chemical composition and mechanical properties of this steel are shown in the following Table 3. The values are chosen from three independent sources, the last one being the EN 10 270-2 standard for hardened spring wires on which Mubea suppliers are based.

Table 3: Chemical composition and mechanical properties of 54SiCr6

Chemical composition								Mechanical properties		Source
C [%]	Si [%]	Mn [%]	P [%]	S [%]	Cu [%]	Cr [%]	Ni [%]	R_m [MPa]	Z [%]	/
0.5 – 0.6	1.3 – 1.6	0.5 – 0.8	-	-	0.3	0.5 – 0.7	max. 0.5	-	-	[12]
0.5 – 0.6	1.3 – 1.6	0.5 – 0.8	-	-	max. 0.3	0.5 – 0.7	max. 0.5	-	-	[28]
0.5 – 0.6	1.2 – 1.6	0.5 – 0.9	< 0.03	< 0.25	< 0.12	0.5 – 0.8	-	1450 – 2050 ¹	min. 40 ¹	EN 10270-2

¹ Quenched and tempered

According to the previous table, it is visible that the chemical composition values do not differ much by sources. The heat treatment parameters for this steel (see Table 4) are:

Table 4: heat treatment parameters of 54SiCr6

Normalizing T [°C] / cooling	Soft annealing T [°C] / cooling	Hardening T [°C] / cooling	Tempering T [°C] / cooling	Source
-	-	min. 840 / oil	375 - 500 / air	[25] (EN 10270-2)
850 - 890 / slowly in the air	710 - 750 / 4 h / furnace	840 - 880 / oil	380 - 580 / air	[28]

This material is widely used in the aerospace and automotive industry. In the automotive industry it is mainly the production of springs that have several uses. These are, for example, suspension springs or springs in belt tensioners [27]. Both types of springs are part of Mubea's production. In this company, the production process runs from winding the wire to the desired spring shape, through heat treatment in the form of stress relief annealing to surface shot peening. This material is subjected to the following research just from the point of view of stress relief annealing.

2.1.2 Specimens A

Mubea's unnamed suppliers supplied spring wires in the form of two independent coils of specific production batches. Inspection certificates were issued for the material supplied, the coils supplied, based on the EN 10204 metallic material standard. Each coil contained a spring wire of different diameter. The diameters were chosen with the greatest difference depending on the availability of coils from the suppliers. Each diameter, each coil therefore has its own inspection certificate, which according to the already mentioned EN 10270-2 standard declares the material properties such as mechanical properties and chemical composition in this particular form (Table 5).

Table 5: Chemical composition and mechanical properties of 54SiCr6 specimens A

54SiCr6	Chemical composition							Mechanical properties	
	∅ [mm]	C [%]	Si [%]	Mn [%]	P [%]	S [%]	Cu [%]	Cr [%]	R_m [MPa]
4.25	0.55	1.45	0.66	0.011	0.005	0.008	0.650	1943*	63*
6.8	0.577	1,377	0,737	0,015	0,012	0,021	0,668	1766*	45,84*

* Quenched and tempered

Wires of uniform length were then cut from the supplied coils (see Table 6). The length was chosen due to the size of the tensile grips and the desired distance between them. The selection of the number of wires is explained below. These wires were then straightened and prepared for heat treatment in the form of stress relief annealing. This heat treatment was followed by experimental research, for example in the form of tensile tests. Finally, some selected specimens were subjected to metallographic analysis. This experimental research and metallographic analysis is described in more detail in chapter 2.3 and 2.4.

Table 6: Wire specimens A

Wire diameter [mm]	Wire length [mm]	Number of wires / specimens [-]
4.25	330 ±2	27
6.8	330 ±2	27

2.1.3 Specimens B: springs

Specimens B were made of the same coil, of the same wire diameter 4.25 mm, where the material properties according to the inspection certificate are given (Table 5). The wire of 6.8 mm diameter could not be used to make the specimens because it was not suitable for the winding process itself and the subsequent tests - measurements in terms of its shape.

Simple springs were bent from the wire to the desired shape using winding tools. Spring dimensions are based on Mubea's internal drawing. This shape was chosen on the basis of suitability for subsequent tests (Figure 16). The spring has 6.029 threads. Thread direction is left.

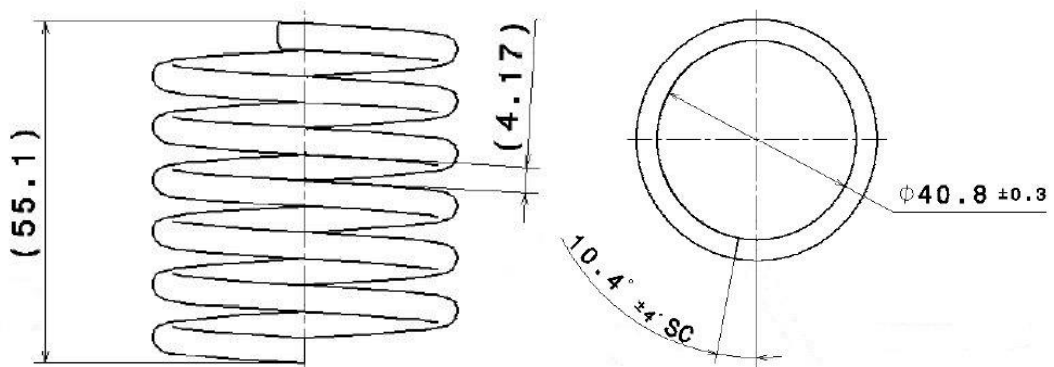


Figure 16: Spring dimensions

A total of 240 springs were made. All of these springs were prepared for heat treatment in the form of stress relief annealing. Before and after heat treatment, see the following chapters, measurements were taken on the springs. Most of them were subjected to a vibration test. Some of them were also shot peened for subsequent durability tests.

Springs were grouped and prepared for subsequent operations (Table 7).

Table 7: Specimens B: springs

Springs: wire 4.25 mm				
Group	1	2	3	4
Number of specimens	52	52	52	52

2.2 Heat treatment – specimens A

For heat treatment purposes of specimens A, the following test plan and test marking were compiled (Table 8). This plan was discussed and designed in accordance with [3], [19], [26] to match the theoretical knowledge of the process (temperature-time) and then, in accordance with the test results, to confirmed, supplement, expand or even disprove the knowledge by the practical findings. The table shows the number of experimental specimens in each series.

This plan was also designed on the basis of the following points:

- 1) The requirement of the company management to perform the heat treatment at a temperature of 420 °C and a time of 20 min
- 2) Actual furnace adjustment at a temperature of 380 °C and a time of 20 min
- 3) Production plant experience with lower temperatures around 300 – 340 °C and with times around 20 – 40 min

The number of specimens was selected primarily for analytical credibility.

Table 8: Test plan and test marking of specimens A

Input wire 4.25 mm (27 specimens)				
Furnace time / temperature	300 °C	340 °C	380 °C	420 °C
20 min	1A	1B	1C	1D
Number of specimens	3	3	3	3
40 min	1E	1G	1H	1J
Number of specimens	3	3	3	3
Without HT	1N			
Number of specimens	3			
Input wire 6.8 mm (27 specimens)				
Furnace time / temperature	300 °C	340 °C	380 °C	420 °C
20 min	2A	2B	2C	2D
Number of specimens	3	3	3	3
40 min	2E	2G	2H	2J
Number of specimens	3	3	3	3
Without HT	2N			
Number of specimens	3			

Heat treatment in the form of stress relief annealing (annealing to reduce residual stresses) of specimens A was carried out at Mubea using a laboratory furnace with silit rods (Figure 17). As already mentioned, the company has also a continuous dual-zone gas furnace. However, for the purpose of this specimens, the first mentioned furnace was chosen because it was possible to set relatively accurate values of temperatures of processes which the temperature regulator achieves with an accuracy of about ± 2 °C.



Figure 17: Laboratory furnace LAC

Heating in the muffle furnace is effected by means of silicon bars which are on its inner sides and are not in direct contact with the atmosphere in the chamber. The furnace also contains type B thermocouples to measure the furnace atmosphere temperature. By means of the thermocouples and the temperature regulator, the heating elements and the furnace atmosphere itself are gradually heated to the selected temperature, with the furnace atmosphere with a certain delay.

Once the selected furnace atmosphere temperature was reached, wire specimens of the two groups listed in the previous Table 8 were placed in the furnace. After the selected time interval, the first group of specimens was removed from the furnace and the heat treatment of the second group continued. Once this process reached its peak also in the second group, the remaining specimens were removed from the furnace. This way (see Figure 18) the other groups of wires were then annealed.

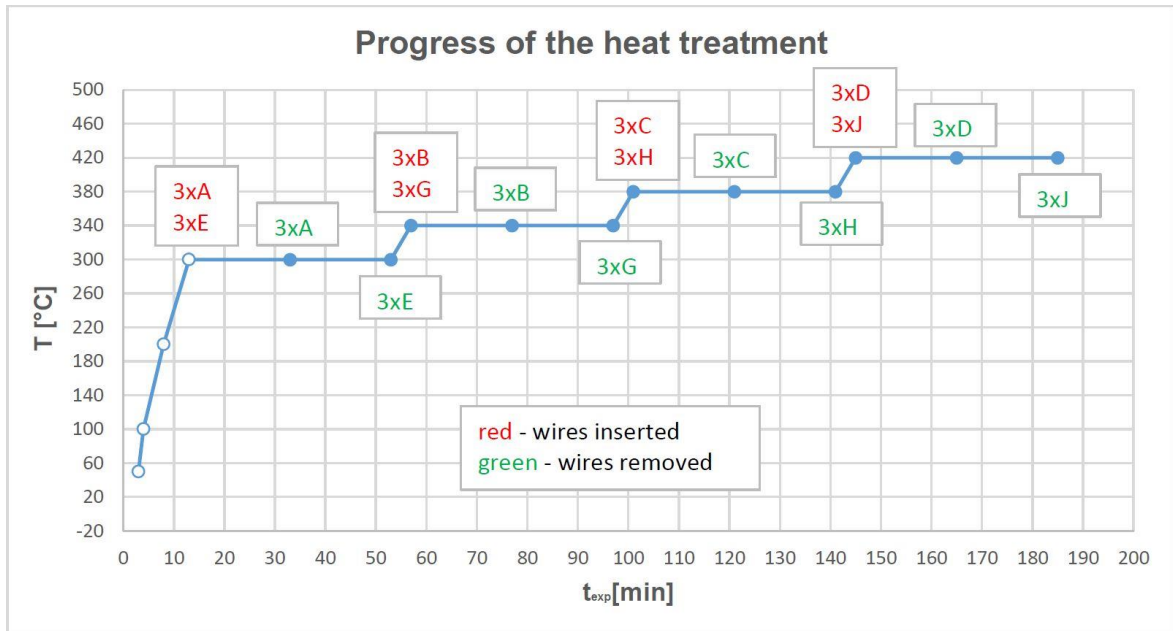


Figure 18: Progress of the heat treatment (t - T dependence of the whole experiment)

Finally, the wires were freely cooled in air after being removed from the furnace. They were properly labelled and stored for later use.

2.3 Mechanical testing methods – specimens A

The object was to compare the individual specimens in terms of temperature-time parameters. The results, the values given in the charts in this chapter are always given for each wire group (for example in terms of heat treatment). The value for each group is calculated by the arithmetic mean A_m of all specimens enriched by corrected standard deviation s . The English literature gives the symbol A as a mark of the arithmetic mean, but because of the use of this symbol already for elongation parameter (chapter 2.3.2), the author of this work started to denote the arithmetic mean as A_m [29]:

$$A_m = \frac{1}{n} \sum_{i=1}^n a_i; \text{ where:} \quad (1)$$

n = number of values, a_i = values

$$s = \sqrt{\frac{1}{N-1} \sum_{i=1}^N (x_i - \bar{x})^2}; \text{ where:} \quad (2)$$

N = number of values, x_i = values, \bar{x} = mean value

2.3.1 Tensile testing

To determine how the material will behave under static load after a certain heat treatment, what its mechanical properties will be, the specimens (see Table 8) were subjected to tensile testing at the Department of Material Engineering using Instron 5582. The tests were performed at room temperature according to EN ISO 6892-1 standard. This equipment is capable of generating a load force of up to 100 kN [30]. This machine was equipped with wedge grips with pneumatic-hydraulic thrust, into which individual specimens were clamped. Prior to clamping, the specimens were labelled with a marker to indicate the free distance between the grips - the original "working" wire length and 100 mm distances to facilitate evaluation of total elongation after the test (Figure 19).



Figure 19: Specimen after testing

Also the diameters of each test specimen had to be measured by calliper before clamping. The values of original diameters and lengths were then entered into the program.

Tensile tests were performed, data were recorded using Merlin software, and specimens were properly labelled and stored for later use. Because no strain gauge (extensometer) was available, the wire extension was calculated by the software as the difference between the final tensile grip distance and the original (free) grip distance. The software also evaluated the dependence of the applied force F [N] on the elongation

ΔL [mm] of a specimen, i.e. $F = f(\Delta L)$. This relationship was then used to create the dependence of the engineering stress R [MPa] on the engineering strain ε [-], i.e. $R = f(\varepsilon)$ in the form of graphs. Furthermore, data such as yield strength at permanent 0.2 % deformation $R_{p0,2}$ [MPa] or tensile strength R_m [MPa] were used [14]:

$$R = \frac{F}{S_0} [\text{MPa}]; \text{ where:} \quad (3)$$

F = applied force [N], S_0 = original cross section [mm]

$$R_m = \frac{F_m}{S_0} [\text{MPa}]; \text{ where:} \quad (4)$$

F_m = a. f. at tensile strength [N], S_0 = original c. s. [mm]

$$R_{p0,2} = \frac{F_{p0,2}}{S_0} [\text{MPa}]; \text{ where:} \quad (5)$$

$F_{p0,2}$ = a. f. at yield strength [N], S_0 = original c. s. [mm]

2.3.2 Tensile test evaluation methods

After all selected specimens were broken, their evaluation was performed, where the resulting comparison of specimens within selected material properties together with discussion are given in chapter 3. The following text focuses only on selected material properties.

The first is the percent **elongation** (overall ductility) of the material. This parameter expresses the percentage ratio of the elongation of the measured length of the test rod after breaking to its original length, denoted by the letter A and calculated as follows [19]:

$$A = 100 \cdot \frac{\Delta L}{L_o} [\%]; \text{ where:} \quad (6)$$

L_o = original measured length, ΔL = increment of original measured length

Due to the use of ratio or non-ratio bars, the designation of ductility by the letter A is supplemented or not supplemented by a subscript. According to EN ISO 6892-1, proportionality coefficients of 5.65 (A) or 11.3 ($A_{11.3}$) are used for ratio bars. For non - proportional bars, the subscript indicates the original measured length of the test bar. The elongation designation $A_{100 \text{ mm}}$ was chosen for the above specimens, which correspond to the non-ratio bars (see ISO 6892-1) [19].

The increment of the measured length of these specimens was read using a simple fixture made on a 3D printer at Mubea (Figure 20).



Figure 20: Mubea simple fixture (made using 3D printing)

Total ductility is a basic parameter given, for example, in material standards. However, it also includes an unusable locally unstable area (leading to neck formation). However, this area is usually undesirable for practical use as it deforms the material in the form of breaking its integrity. For this reason, the plastic ductility value A_g , which gives the maximum uniform deformation without local reduction of the cross-section, is more decisive [14], [19].

Using the same fixture, see Figure 20, **the reduction of area** (contraction) was evaluated, respectively the cross-section of the broken sample was measured. The reduction of area Z gives the percentage ratio of the difference between the original and the broken cross-section of the test sample to its original cross-section. It is calculated as follows [14], [19]:

$$Z = 100 \cdot \frac{\Delta A}{A_o} [\%]; \text{ where:} \quad (7)$$

A_o = original cross – section area [mm²],

ΔA = difference between original and broken cross – section area [mm²]

Material plasticity was also evaluated. Plasticity indicates the ability of a material to deform with respect to the ambient temperature, where the deformation is not affected

by any other factor. On the other hand, formability is defined, where the material is already affected by several aspects in the whole technological forming process [14], [19].

The plasticity of a material is usually evaluated in several ways, such as total ductility, ratio of yield strength to tensile strength, or plastic anisotropy size. However, these methods have disadvantages. The overall ductility depends on the original measured length of the rod, the method of determining the ratio of yield strength to tensile strength or the method of determining the size of plastic anisotropy is not very effective [14], [19].

A suitable solution seems to be the method of calculation of the **Plasticity stock PS**, where the plasticity is evaluated energetically. Generally, the energy (work) required for permanent deformation is the product of force and change of position. Both of these quantities appear in the tensile test in the form of acting force and elongation. The plasticity stock assuming a featureless yield strength is then calculated according to the formula [19]:

$$PS = 0,75 \cdot (R_m - R_{p0,2}) \cdot \varepsilon_g [\text{MPa}/\text{Nmm}^{-2}/10^{-3}]\text{mm}^{-3}]; \text{ where:} \quad (8)$$

$$\varepsilon_g = \text{permanent engineering strain (permanent ratio elongation)} [-]$$

This calculation is a numerical representation of the graphical area in the area of permanent deformations within the tensile diagrams with featureless yield strength, starting from the yield strength $R_{p0,2}$ and ending with the tensile strength R_m with respect to the permanent elongation at these two values (Figure 21) [19].

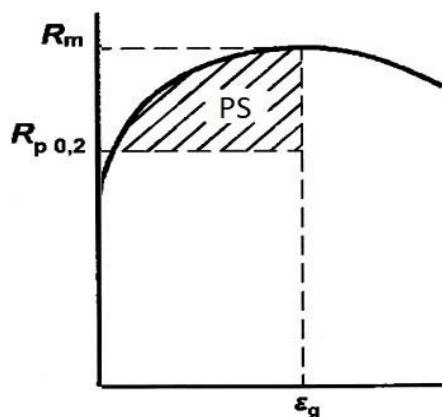


Figure 21: Graphical area of PS (Plasticity stock) [19]

2.3.3 Modified impact test

However, the static tensile test results do not give information about the dynamic behaviour of the material. Dynamic stress is very noticeable in technical practice, when working with springs. The forces to be achieved for material failure of a component under this type of loading are not nearly as high as those under static loading. When the loading force increases by a jump, an impact load is created. With repeatedly changing loads, cyclic loads are generated.

The most commonly used bending impact test is the Charpy test according to EN ISO 148. For these test methods, specimens with a basic dimension of 10 x 10 x 55 are prepared. These specimens are also provided with a V-shaped or U-shaped notch in the middle of their length, where the use of a V-notch is more common. This test method is performed on a Charpy pendulum hammer. The principle of the test is to break the test specimen supported at both ends with a notch located on the opposite side of the hammer impact point [14], [19].

In this case, the modified impact bending test was used, which could not be further specified due to the patent application. This test is similar to the Charpy method.

The specimens were provided with a V-notch using the CNC milling machine - Emco Concept Mill 55. The notch with an opening angle of 45° was made exactly to the half of the sample cross-section due to subsequent calculations. For the purpose of notch milling, the company made a special fixture or pairs of fixtures for each wire diameter. (Figure 22).

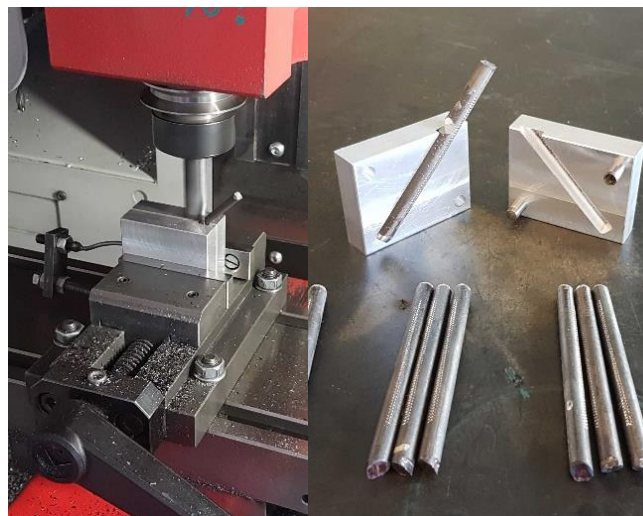


Figure 22: EMCO Concept Mill 55 and specimen fixture

2.3.4 Vickers microhardness test

The last mechanical test performed on specimens A was the Vickers microhardness test based on EN ISO 6507-1. Under this name this method is known in Europe. In the US, it is called the diamond pyramid hardness test.

It is a static microhardness test, where the indenter is pressed by a calm force in a direction perpendicular to the tested surface. This penetration test is often used for its accuracy, simplicity and good reproducibility. Resistance to foreign body penetration is determined by the magnitude of forces with which the metal atoms are bound to each other. In a metal bond, which allows plastic deformation, deformations become easier as the bond forces are more balanced. The shape of the crystal elements, the fineness of crystallization, temperature, foreign matter and internal stresses are important factors. The temperature at which the tests are carried out is between 10 and 35 °C. In arbitration cases, the tests shall be carried out at a temperature of 23 ± 5 °C [31].

This method of testing the hardness or microhardness as test specimen utilizes a quadrilateral diamond pyramid with a top wall angle of 136 °. The choice of this angle was chosen to minimize friction between the indenter and the material in the indentation area. At the same time, it wanted to be achieved similarity of the resulting values between this test and the Brinell hardness test [31].

This time, however, the tests were not performed on all specimens A, but only on a few selected ones. The decisive factor was the result of the tensile tests, on the basis of which the representatives with the highest and the lowest strength were chosen (Table 9).

Table 9: Test plan of selected specimens A

HV1 (9,8 N): input wire 4.25 mm + 6.8 mm				
Furnace time / temperature	300 °C	340 °C	380 °C	420 °C
Without HT	1N + 2N			
Number of specimens	3 + 3			
20 min	/	1B + 2B	/	/
Number of specimens	/	3 + 3	/	/
40 min	/	/	1G + 2G	1J + 2J
Number of specimens	/	/	3 + 3	3+ 3

2.4 Metallographic analysis – specimens A

Specimen preparation and observation took place in the metallography laboratory at the Department of Material Engineering of the CTU, Faculty of Mechanical Engineering in the following order.

Selected specimens, see Table 9, were cut into 10 – 15 mm pieces on the Leco MSX-255. These pieces were modified on a disc grinder and further equipped with special clamps for their subsequent pressing (Figure 23).

Pressing of the pieces was performed in metallographic mounting press Leco PR4X using black phenolic resin. The diameters of the resulting samples were 30 mm (Figure 23).

The molded samples were then grind on traditional abrasive papers with a grade of P220 and P1200 based on silicon carbide using the Leco GPX300. The grinding was followed (in the same equipment) by polishing the samples on polishing pads, which were moistened with wetting agents. For the purpose of polishing, a diamond monocrystalline suspension of 3 µm as well as a SiO₂-based solution were also used (Figure 24). After achieving optimum surface roughness, samples were placed in a Neophot 32 light microscope and microstructure images were taken using the enclosed software.

The last step of sample preparation was their etching with 98 % ethanol and 2 % nitric acid solution. After this step, a surface relief of the microstructure was formed. This way treated samples were re-inserted into a Neophot 32 light microscope to observe and document the structure of the etched material.



Figure 23: Leco MSX-255; special clamps; Leco PR4X



Figure 24: Leco GPX300 - samples polishing

2.5 Heat treatment – specimens B

In this chapter, in addition to the heat treatment process itself, testing of specimens B is given because of the interconnection of these processes.

2.5.1 Stress relief annealing, testing and measurement

Prior to the heat treatment process, each of the springs (specimens B) was measured after winding and entered in a table that is not given due to the amount of data. The angle was measured using a device as shown in Figure 25.



Figure 25: Angle measuring device

After measuring the angles, the springs in groups 1-4 (see Table 7) were threaded onto thin wires. A total of 4 spring bundles were available.

At the same time, the following plan was drawn up (Table 10). This plan has been discussed and designed to be consistent with the theoretical knowledge of this process and to be directly related to the plan for specimens A, see Table 8.

Table 10: Heat treatment plan for specimens B

Springs: wire 4.25 mm				
Furnace time / temperature	300 °C	340 °C	390 °C	410 °C
20 min	bundle 1	bundle 2	bundle 3	bundle 4
Number of specimens	52	52	52	52

This was followed by a heat treatment in the form of stress relief annealing of the specimens B. The annealing was carried out in Mubea using a continuous dual-zone gas furnace. Individual bundles of springs were gradually inserted into a continuous furnace

and annealed at selected temperatures for 20 minutes (Table 10). Attention is drawn to the fact that the temperature in the spring-processing furnace differs slightly in two cases from the temperature used in the laboratory heat treatment of specimens A. It should also be noted that in all cases the temperature variance of ± 40 °C was detected. The position of the spring on the conveyor belt has an influence on the temperature and the temperature also differs in terms of the location of the furnace passage. The author is aware that this may affect the results of specimens B. However, for a general assessment of the effect of heat treatment on the properties of 54SiCr6 steel, it is appropriate to use these results.

After the heat treatment, the angle of each of the springs was measured again and entered in the same table as in the previous measurement.

Finally, the aligned springs were again threaded onto the wires and placed in a vibration bath. This time, however, only in limited quantities, as some of them had planned other measurements and tests. The vibration process was included in the tests because of the possible prediction of residual stresses after the previous stress relief annealing, as this process is one of the possibilities to reduce residual stresses [32]. Vibration parameters together with the number of specimens are in the following Table 11.

Table 11: Vibration parameters with the number of specimens

Springs: wire 4.25 mm				
Vibration bath	Frequency: 35 Hz; time: 30 min			
Bundle	1	2	3	4
Number of specimens	50	50	50	50

On the springs removed from the vibration bath, their angle was again measured and entered in the aforementioned table.

The results, the values given in the charts in the following chapter 3 are always given for each wire group (for example in terms of heat treatment). The value for each group is calculated by the arithmetic mean A_m (1) of all specimens enriched by corrected standard deviation s (2).

2.6 X-ray diffraction – specimens B

Due to the fact that the angles after the vibration bath have not changed, it can be assumed that the vibration does not change the residual stress at given parameters. For this reason, X-ray diffraction was only performed on specimens B after heat treatment, see the following chapter 2.6.2.

2.6.1 Residual stresses

X-ray diffraction diagnostics of surface layers of machine parts is important in the field of residual stress measurement. Residual stresses accompany every technological process in which plastic deformation occurs under mechanical load. These deformations are easiest in surface layers because they are not limited by the strong bonding of the surrounding crystals. The deformations are performed by slipping in the region of favourably oriented crystals. After release of the surface layer, further layers are gradually released [3], [33].

The process of winding the wire into the shape of a spring is based on the same principle. Along with the deformations, stresses occur in the wire cross-section. Basically, due to deformation, tensile stresses occur on the outside of the spring and compressive stresses occur on the inside of the spring. The deformations in the wire cross-section are plastic but also elastic. The distribution of stress under purely elastic loading is shown in Figure 26. The elastically deformed area tries to return to its original state, while exerting pressure on the plastically deformed layer (Figure 27). This results in a compressive stress in the surface layer on the outside of the spring, which decreases towards the wire axis. At a certain point it reaches zero and beyond this point there is a tensile stress. The inner side of the spring has the opposite character, where the resulting tensile stress occurs in the surface layer (Figure 28). At re-loading the stress distribution is shown in Figure 29 [3], [33].

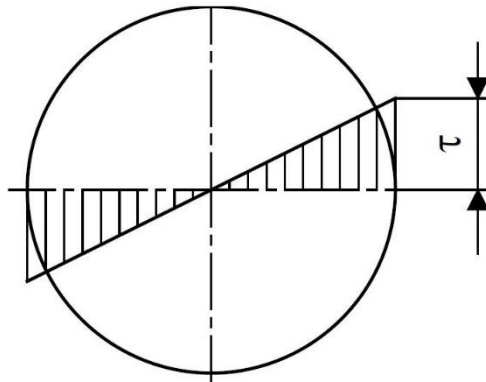


Figure 26: Elastic deformation

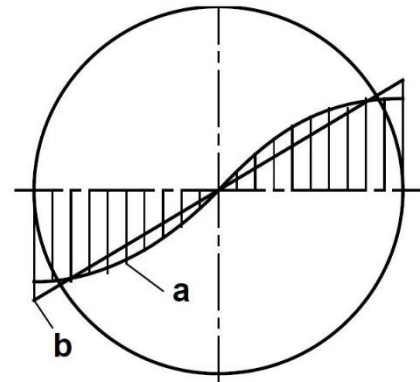


Figure 27: Elastic and plastic deformation
(a - load, b - suspension)

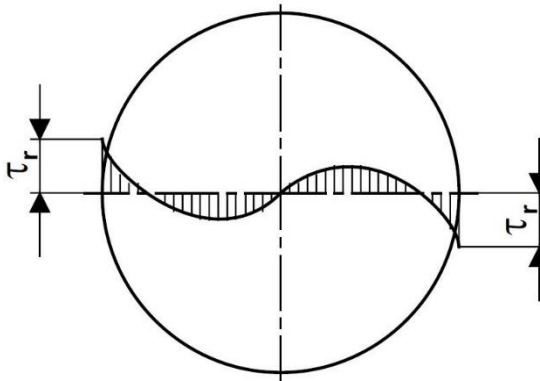


Figure 28: Difference between load and suspension

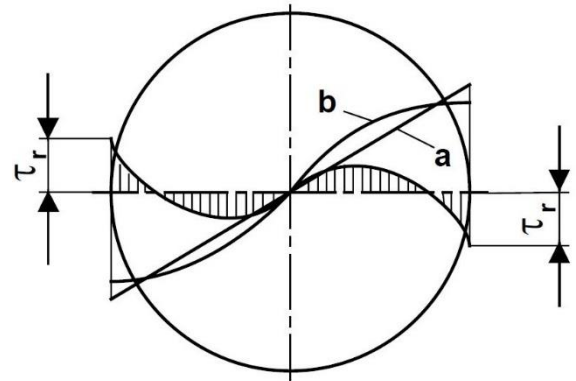


Figure 29: Re-loading

2.6.2 X-ray strain gauging

The essence of X-ray strain gauging is the use of X-ray scattering (diffraction) on crystals to measure the variations in the distances of atomic lattice planes induced by stress [34].

One of the practically significant peculiarities of X-ray strain gauging is that the surface of the examined material does not need to be specially treated before the measurement. A roughness usually encountered after machining or forming is not a problem. However, it is always necessary to consider the implications of the depth of penetration of the X-rays used for the task [34].

The dependence of the stress tensor components σ_{ij} on the distance T from the surface can often be more important than the surface values $\sigma_{ij}(0)$ for predicting

the strength properties of the product. Knowledge of the function $\sigma_{ij}(T)$ enables to predict the operational reliability of the product, resp. select a suitable surface treatment to create the required thickness and sufficient pressure prestressing of the layer representing a barrier to cracks going from the surface to the inside of the volume. From an economic point of view, the objective is to optimize the manufacturing technology so that the surface provides reliable protection against product breakage even if cracks reaching certain subcritical values are observed [34].

For a Fe-based material, X-ray radiation with a chrome anode is suitable for diffraction analysis of stress inhomogeneities (the course of residual stresses that change significantly in a few tens of μm below the surface). Due to the high absorption, $\text{CrK}\alpha$ beams penetrate only to a small depth ($\approx 100 \mu\text{m}$). The measured stresses are therefore surface specific. The dependence $\sigma(T)$ can be obtained as a graph of stress values σ assigned to the distances T from the original surface to the surfaces, which are gradually electrolytically exposed at a selected place of the examined sample [34].

The objective of this assignment was to determine the depth profile of the residual stress on specimens taken from the annealed screw springs (Table 12). Specimens were always taken from the middle part of the spring.

Table 12: Specimens for X-ray diffraction

Springs: wire 4.25 mm				
Furnace time / temperature	300 °C	340 °C	390 °C	410 °C
20 min	spring 1	spring 2	spring 3	spring 4
Number of specimens	1	1	1	1

As can be seen from the table, only one sample was selected from each heat treatment group because of the cost of this analysis.

Strain gauge measurements were performed using a single exposure method without reference substance with diffracted radiation detection on a memory film combined with sequential electrolytic etching. For each specimen formed by the cut from the spring, one spot on the inner surface in a direction perpendicular to the inner fibre was analysed (Figure 30).

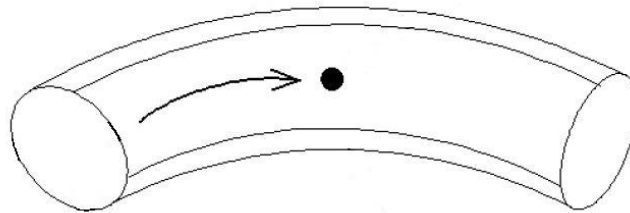


Figure 30: The spot of analysing residual stresses

To verify that there was no significant stress release during specimen formation, the residual stress on the outside of the specimen before and after formation was measured. The measurements were performed by Mubea in Germany. The test parameters are given in Table 13:

Table 13: Test parameters

Device	Bruker D8 Advance
Operation mode	Ω - Stress
Radiation	Cr-K α
Used lattice plane	bcc {211}
Collimator diameter	1 mm
Used Ψ (psi) angle	-45°, -33.75°, -22.5°, -11.25°, 0°, 11.25°, 22.5°, 33.75°, 45°
Evaluation method	$\sin^2 \Psi - 2\Theta$
Young's modulus	220.000 MPa
Poisson's ratio	0.28
Sample angle ϕ (phi)	0°
Measurement position	Inner diameter/ middle of spring (see overview)

The results, the values given in the charts in the following chapter 3 are always given for each wire group (for example in terms of heat treatment). The value for each group is calculated by the arithmetic mean A_m (1) of all specimens enriched by corrected standard deviation s (2).

2.7 Durability test – specimens B

Together with X-ray diffraction analysis, durability tests were performed on selected specimens B. These tests are used by Mubea to test / verify newly designed springs. In one test setup, four springs were tested at the same time. The result of these tests is the number of cycles until spring failure.

The following Table 14 shows the processing parameters of the tested springs.

Table 14: Specimens for durability test

Springs: wire 4.25 mm				
Furnace time / temperature	300 °C	340 °C	390 °C	410 °C
20 min	spring 1	spring 2	spring 3	spring 4
Number of specimens	1	1	1	1

The tests were carried out using a special Mubea testing machine that quickly simulates the behaviour of the spring in operation. The process parameters were 33 Hz frequency and 21 ° oscillation amplitude.

2.8 Overview of specimens, tests and measurements

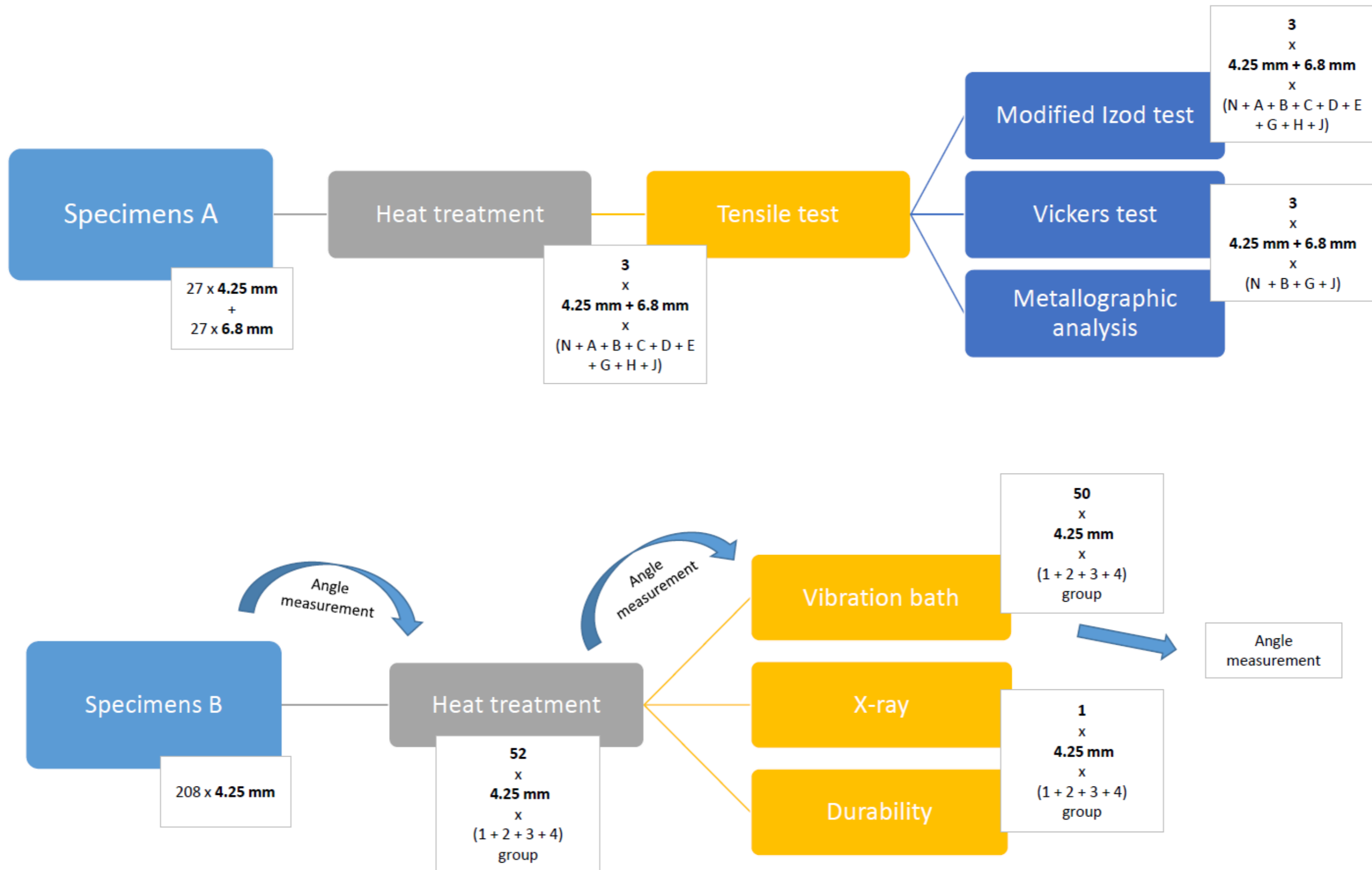


Figure 31: Overview of specimens, tests and measurements

3 Results and discussion

The aim of stress relief annealing is to eliminate internal stresses as much as possible while maintaining the mechanical properties of the material. The same was the subject of this thesis. Several tests were carried out on wires and springs to determine optimal parameters of the annealing process. The object was to compare the individual specimens in terms of temperature-time parameters.

3.1 Mechanical testing methods – specimens A

Due to the extent of the experiments, the results are presented and discussed separately for specimens A and B.

3.1.1 Tensile testing

On the prepared samples, cut wires annealed in the laboratory muffle furnace, the tensile test was performed first. Figure 32 shows the engineering stress-strain diagrams $R = f(\varepsilon)$ for all monitored states and both wire diameters.

From the results of the 4.25 mm wires, it can be concluded that at 420 °C the strength characteristics decrease and the material ductility increases. The difference between the annealing times is also visible for this temperature. The decrease in strength and the increase in ductility at this temperature appear to be due to the tempering of the steel, which for 54SiCr6 begins at 375, respectively 380 °C, see Table 4 [25], [28], [35], [36].

In the non-heat treated wire, there is also a visible difference compared to the annealed wire, where the strength characteristics are lower and the ductility is higher except for the temperature of 420 °C. An increase in strength characteristics and a decrease in ductility at 300 and 340 °C could be attributed, due to the content of carbide-forming elements in the material, certain sensitivity of the material to precipitation hardening [21], [23], [35], [37]. This process, or the influence of individual elements, should be further explored in relation to the submitted work.

For other wires the values are much more comparable. There is a noticeable difference between annealing at 380 °C compared to 300 and 340 °C, where there is a certain decrease in mechanical properties at 380 °C. The difference between 300 and 340 °C appears to be insignificant in terms of temperatures. However, one could conclude that the time of annealing is more decisive there.

From the results of the tests on 6.8 mm wires it can be seen at first glance that the mechanical properties are significantly more stable than the 4.25 mm diameter. Compared to the 4.25 mm wire, there is a visible decrease in strength. At the same time, there is a higher material ductility. This stability and different mechanical properties could be attributed to differences in production between suppliers. However, these differences could not be further investigated due to manufacturing secrets.

A wire with a diameter of 6.8 mm appears to have lower strength and, at the same time, higher ductility in the state without heat treatment along with the wire annealed to 420 °C. There is a visible difference in ductility between the temperature of 420 °C and the state without heat treatment. At 420 °C there is also some difference in the annealing time. There appears to be some effect of tempering too.

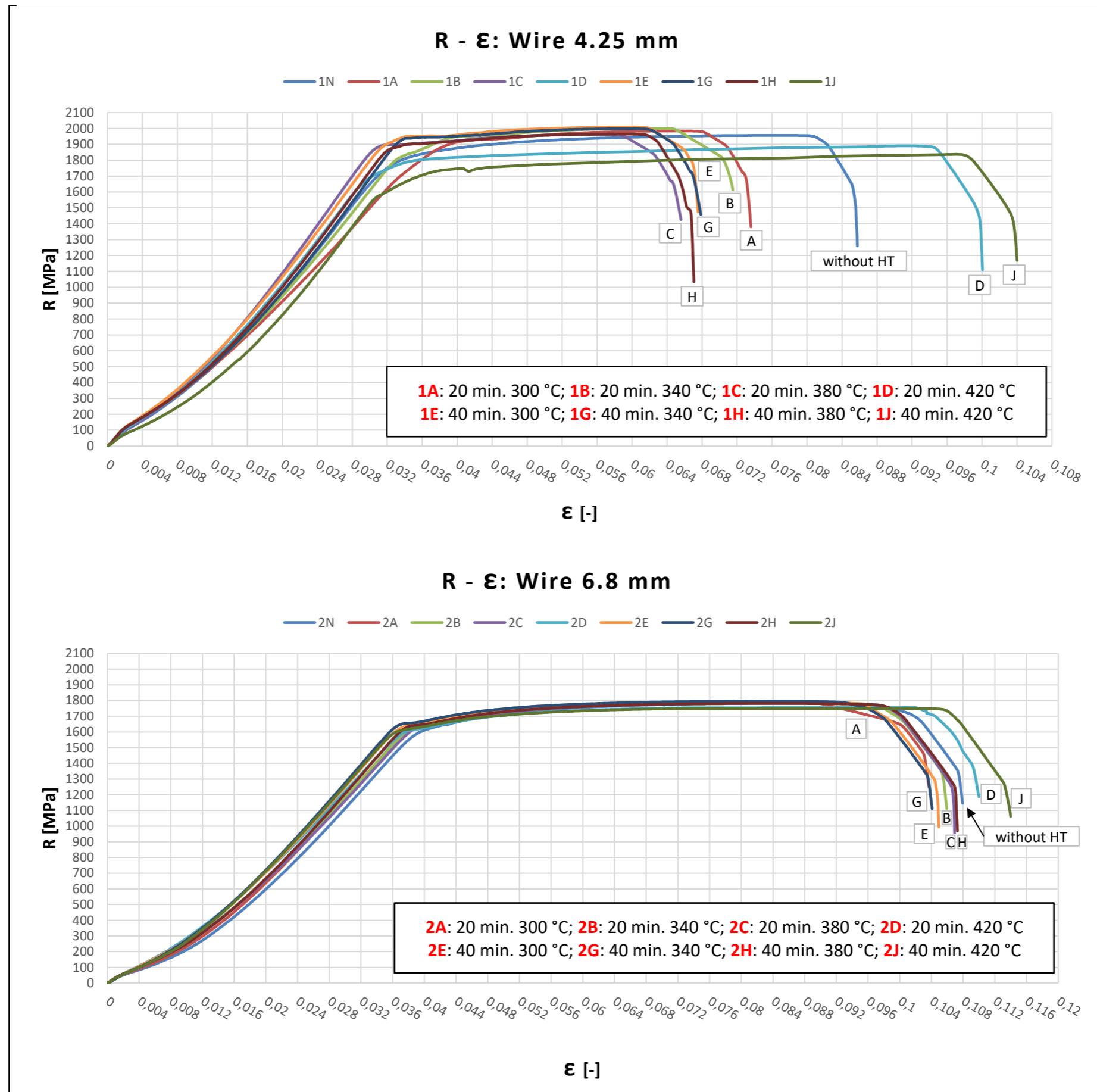


Figure 32: Graphical dependence $R - \epsilon$

3.1.2 Strength and hardness parameters (R_m , $R_{p0.2}$, HV1)

Along with the graphical dependence $R = f(\varepsilon)$, another graphical dependence was constructed (Figure 33), which provides an overview of the strength characteristics and HV1 hardness measurements. Although the strength of the wires complies with the inspection certificate for both diameters, results cannot be compared due to different suppliers. Following this work, it would be appropriate to supplement the results with tests for both wire diameters from one supplier.

With respect to 4.25 mm wires, it could be concluded that for the annealing temperatures of 300 - 340 °C, the values of the tensile strength R_m increase compared to the non-annealed condition. While the R_m at these temperatures increases in the order of magnitude, $R_{p0.2}$ increases significantly more. At 380 °C, the R_m return to the original value (without heat treatment), while the $R_{p0.2}$ remains one order of magnitude higher than the original condition. There you can see some difference in temperature settings without any expressive time setting significance. However, this is not entirely true for a temperature of 420 °C, where a significant decrease in R_m and $R_{p0.2}$ can be seen from the graph, as well as a difference in the setting of the processing time.

A similar character could be attributed to wires with a diameter of 6.8 mm, where the differences are not as large as for wires 4.25 mm. From the tensile strength graph for this diameter, it can be concluded that the annealing time together with the selected temperatures has no significant effect on this mechanical parameter. This fact is in accordance with theoretical assumptions [3], [21], [26]. It is desirable that the stress relief annealing does not lead to a decrease in the strength of the spring wire.

The differences in tensile strength and yield strength could be attributed to the formation of precipitates in the structure of the material and the process of tempering. The differences in mechanical values between the diameters and the overall stability of the values for the 6.8 mm wire seem to be (based on the previous chapter) because of the different production between suppliers.

For a wire diameter 4.25 mm in terms of yield strength $R_{p0.2}$, the most suitable heat treatment temperature in the form of stress relief annealing seems to be 300 - 340 °C. Something similar could be stated about the tensile strength R_m .

For a wire diameter 6.8 mm in terms of R_m and $R_{p0.2}$, a temperature of 420 °C should be avoided.

The Vickers HV1 (load 9.8 N) microhardness curve for selected specimens corresponds to the strength curve, with both wire diameters at the highest value for annealed wire at 340 °C and the lowest for annealed wire at 420 °C. The wires without heat treatment have an average HV1 hardness value. The microhardness of the 6.8 mm wire seems to be lower than of the 4.25 mm wire, which is in accordance with R_m (Figure 33).

Differences in hardness between wires could be justified in a similar way to the tensile strength in the previous chapter. Annealing at 340 °C seems to be more suitable from the microhardness point of view than the non-annealed state or annealed state at 420 °C.

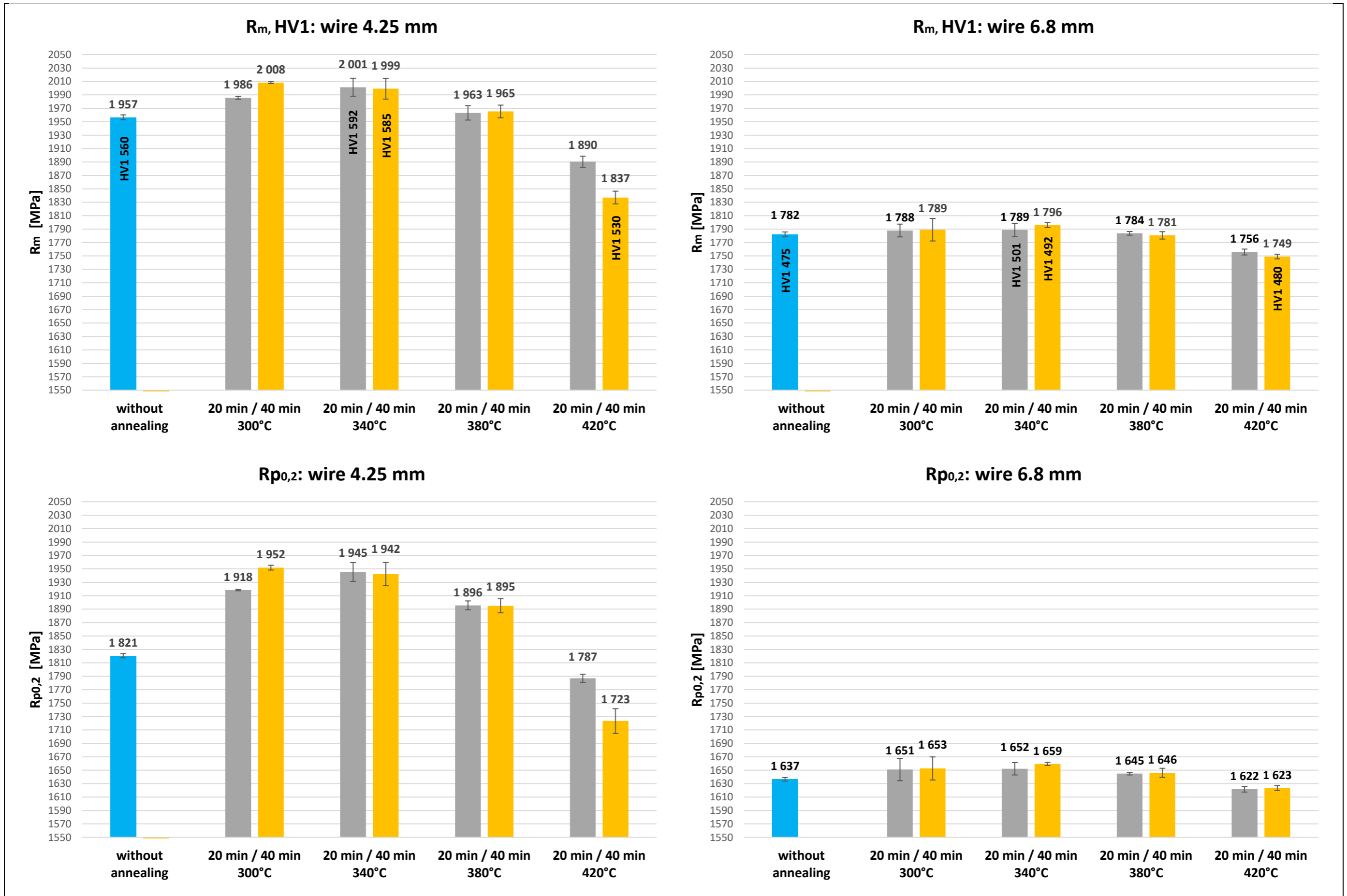


Figure 33: Graphical dependence R_m, R_{p0,2}, HV1 – heat treatment

3.1.3 Ductile characteristics ($A_{100\text{ mm}}$, Z)

The ductile characteristics of the monitored states are shown in Figure 34. The ductility results for a diameter of 4.25 mm correspond to the results of the strength characteristics (Figure 33), but are significantly distorted by the measurement (observational) error. The contraction results for a diameter of 4.25 mm do not appear to be consistent with the results in Figure 33, which could also be due to a measurement error.

The results for a diameter of 6.8 mm appear to correspond to the strength characteristics with respect to the considerable measurement error.

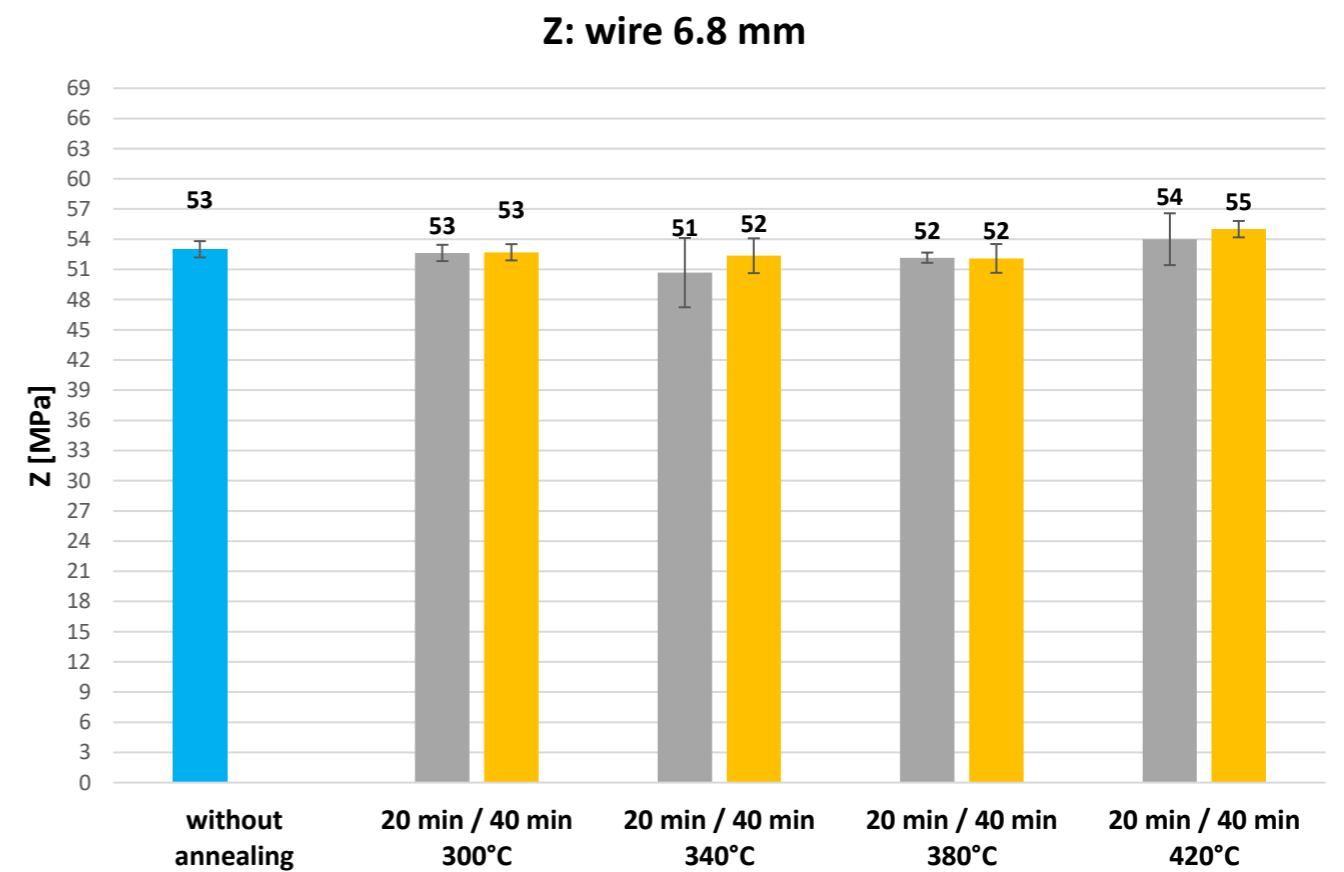
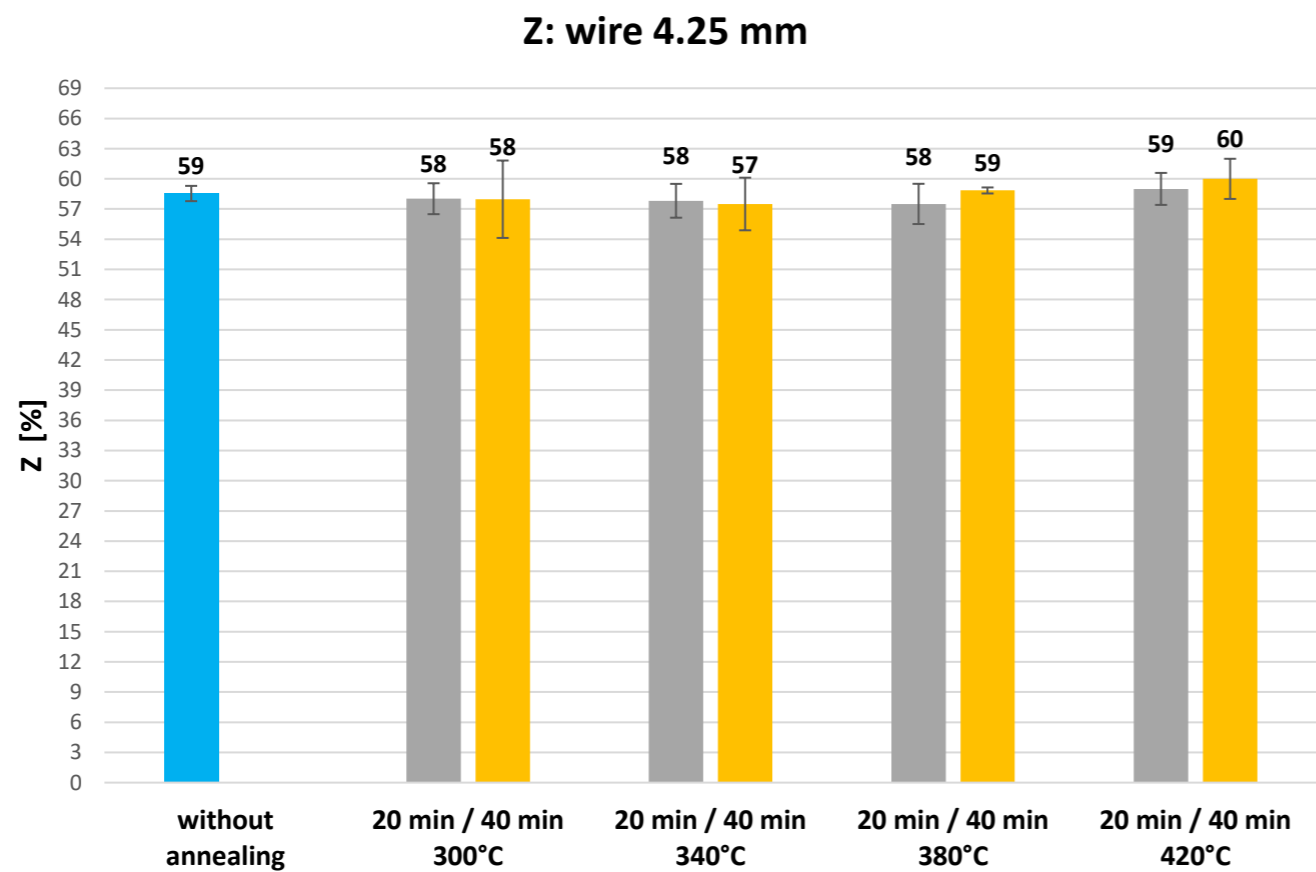
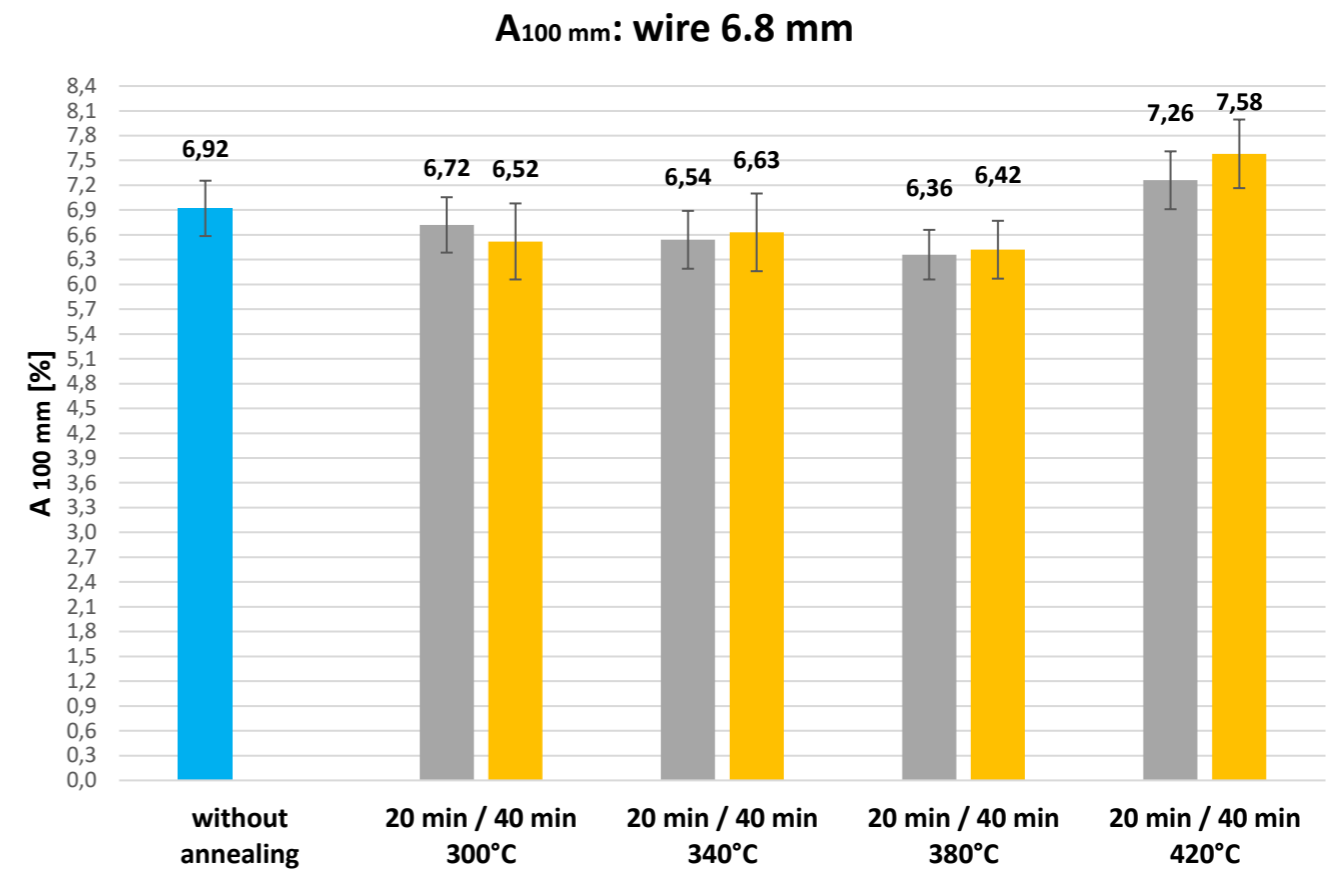
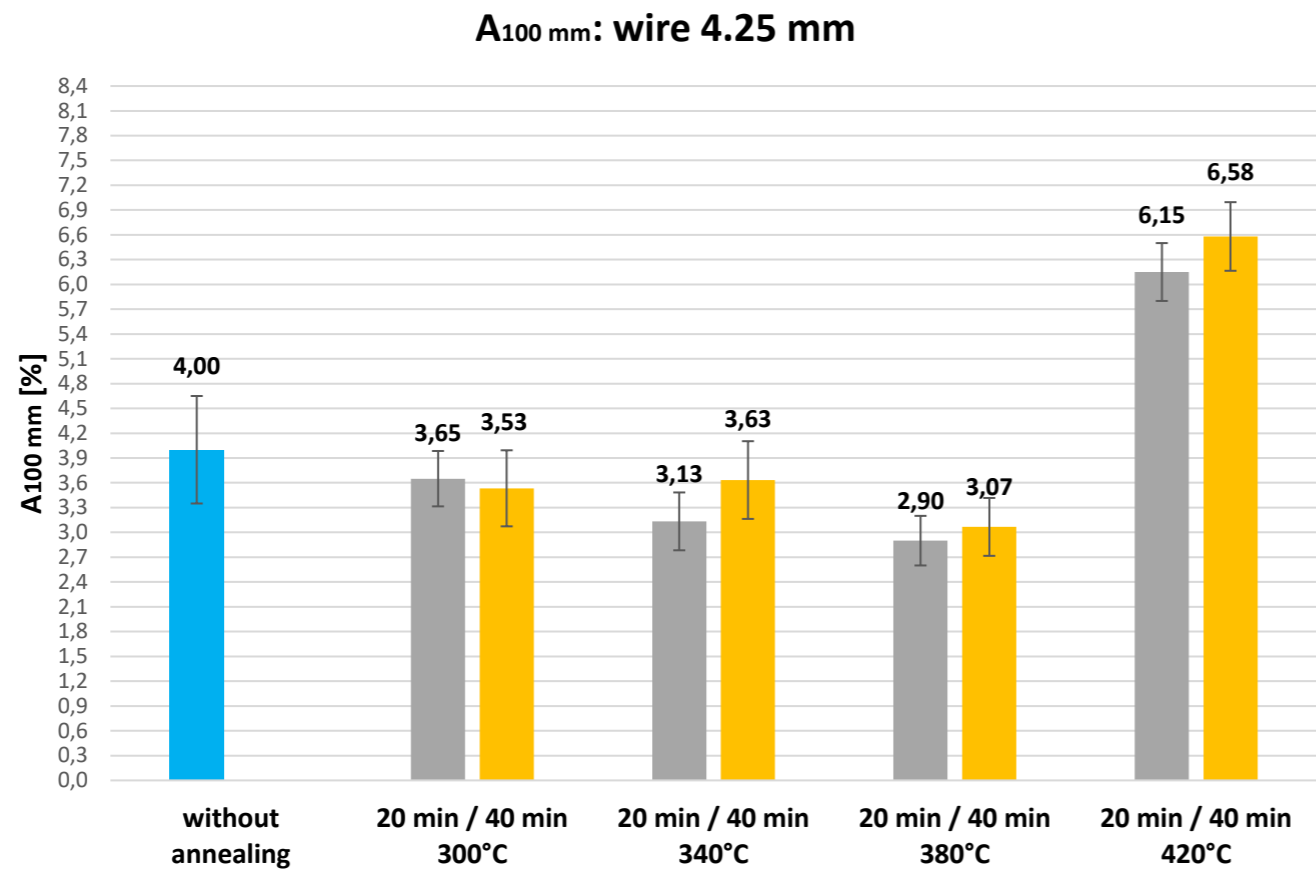


Figure 34: Graphical dependence A_{100 mm}, Z – heat treatment

3.1.4 Plasticity stock (*PS*) and toughness parameter (λ)

Figure 35 shows the dependencies of the ductility parameters of the monitored states. This is the plasticity stock (*PS*) and toughness parameter (λ) that was obtained by the modified impact test.

It is apparent from the *plasticity stock* values that the annealing temperature of specimens with a diameter of 4.25 mm has an influence on the achieved *PS*. Compared to the material without annealing (initial state), after annealing at temperatures of 300 to 380 °C, a decrease in the *PS* was found, which corresponds to the strength and ductility characteristics in the previous chapter. Annealing at 420 °C caused an increase in the *PS*, which is more pronounced with longer annealing time (40 minutes). In the temperature range of 300 to 380 °C, the effect of the annealing time in the range of 20 to 40 minutes has not been demonstrated. The character of the dependence of *PS* on the annealing parameters is in good line with the character of this dependency for ductility.

A similar trend, but with minor differences, have results of 6.8 mm specimens, with annealing causing a slight decrease in the *PS* except the temperature of 420 °C.

The results of the toughness parameters are of a similar nature to the results of the *PS*, which corresponds to the theoretical assumption [19], [23].

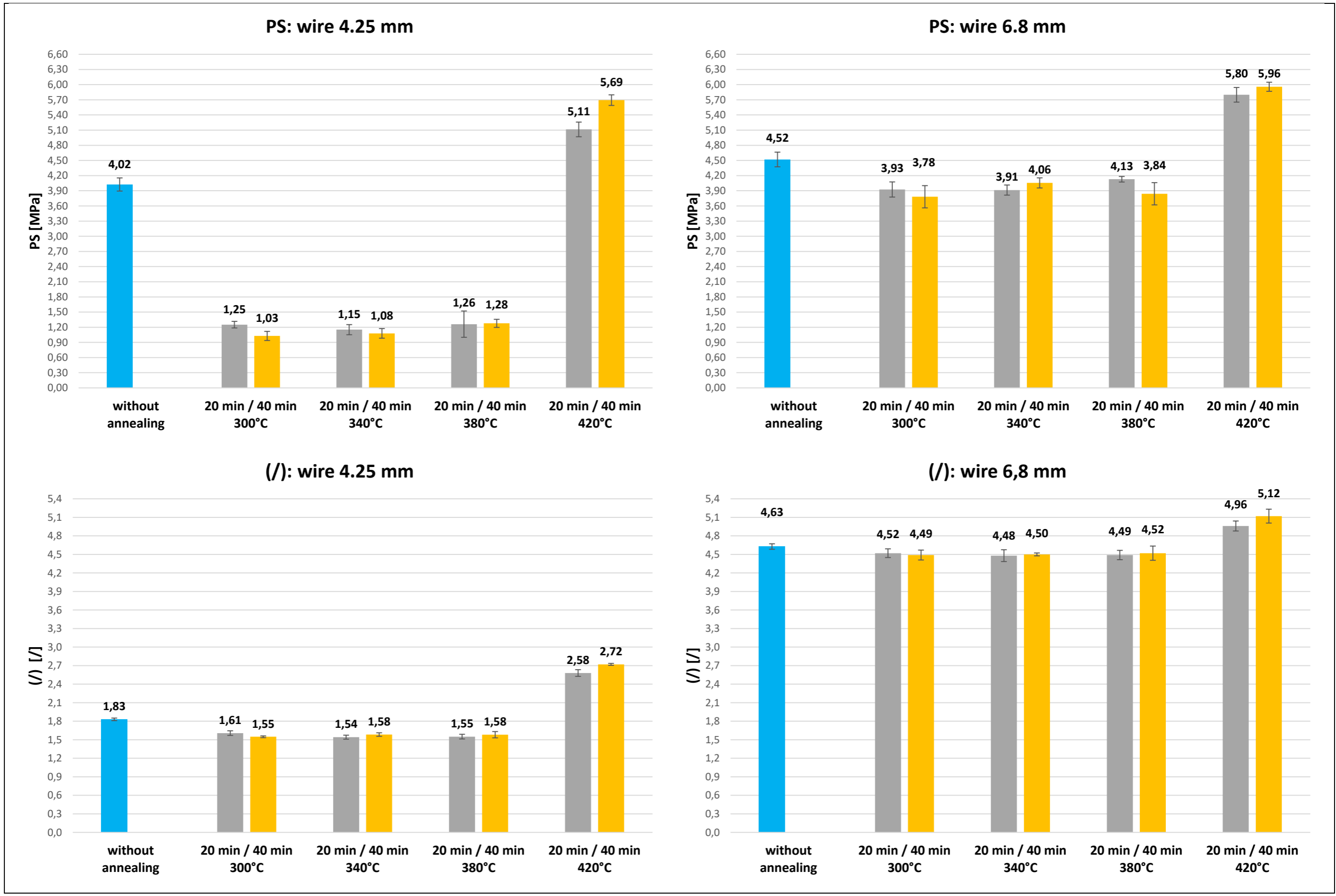


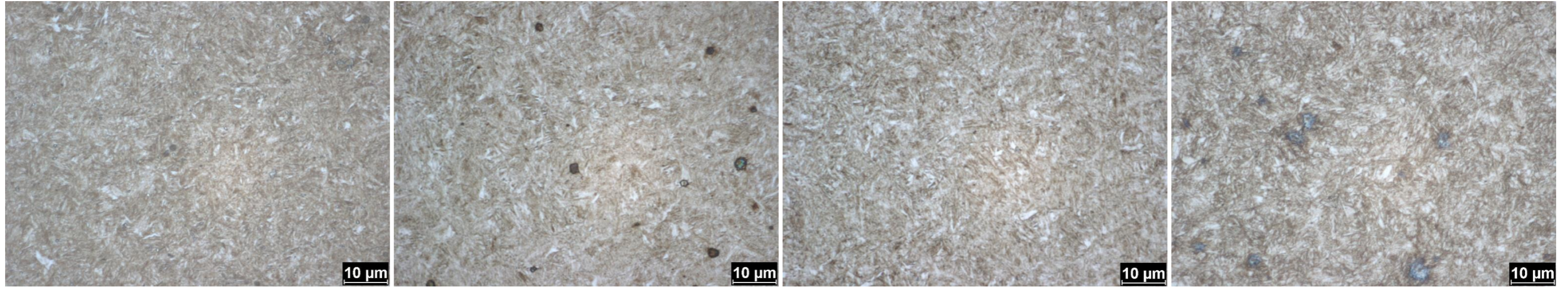
Figure 35: Graphical dependence PS, W – heat treatment

3.2 Metallographic analysis – specimens A

Images from the metallographic analysis are shown in Figure 36.

The comparison of the structure of specimens without heat treatment diameter of 4.25 and 6.8 mm shows a difference that is in good line with the different properties of the monitored specimens. It can be seen from the Figure 36 that the structure of the initial state (i.e. delivered state quenched and tempered) is coarser for a 6.8 mm wire than for a 4.25 mm wire. This is in good line with the fact that the wire strength of 6.8 mm is significantly lower than that of the wire 4.25 mm. In both cases, the structure is formed as expected with sorbitol. A small proportion of residual austenite can be expected which cannot be detected by light microscopy. In general, in accordance with the theoretical assumption of stress relief annealing, there was no fundamental change in structure [19], [23]. The structures after annealing at 340 °C for 20 and 40 minutes do not differ when viewed by light microscopy. When comparing the structures after annealing at 340 °C for 40 minutes and at 420 °C for 40 minutes, it can be stated that the structure after annealing at 420 °C for 40 minutes is slightly coarser for both wire diameters. The facts described are in good line with the tensile test characteristics.

Magnification: 50 x 16 – 4.25 mm wires



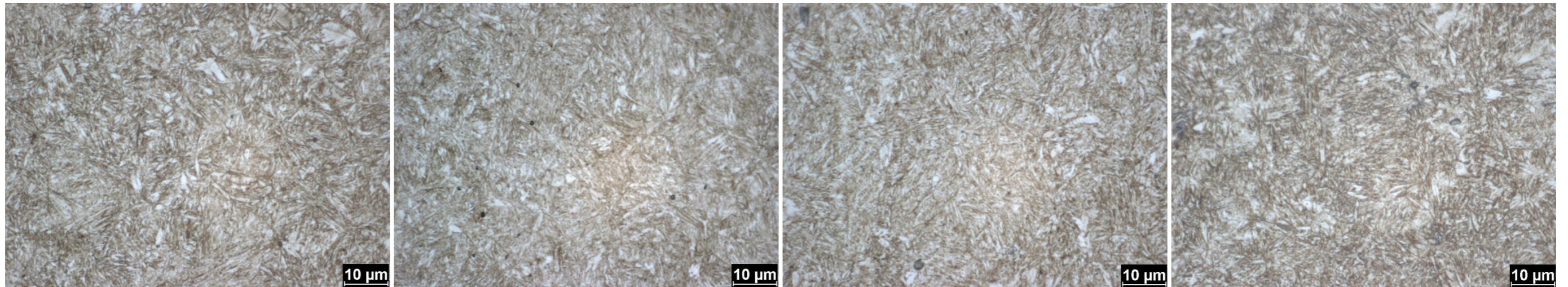
Without heat treatment

340 °C – 20 min (1B)

340 °C – 40 min (1G)

420 °C – 40 min (1J)

Magnification: 50 x 16 – 6.8 mm wires



Without heat treatment

340 °C – 20 min (2B)

340 °C – 40 min (2G)

420 °C – 40 min (2J)

Figure 36: Metallographic images of specimens A

3.3 Winding angle measurements – specimens B

From the results of the angles measurements on the made springs, the differences in the angles after stress relief annealing are visible. The winding process appears to be stable (Figure 37). Figure 37 also shows the effect of the vibration bath to determine or predict residual stresses after annealing, which seems to be negligible at the selected parameters.

The differences in the angles between the winding and the annealing are higher with increasing temperature, while the values are less stable. Annealing at 300 and 340 °C appears to be the most stable (due to corrected standard deviation). Based on these results, it can be assumed that with increasing annealing temperature there is a significant reduction in internal stress.

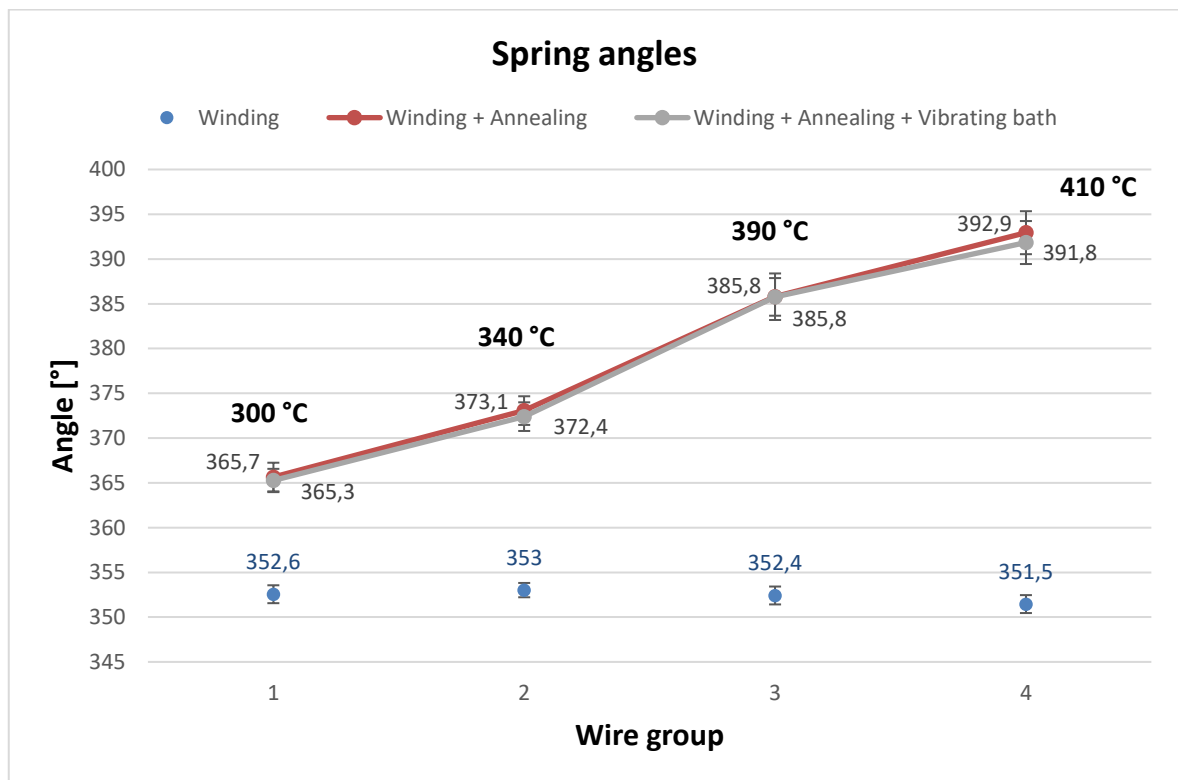


Figure 37: Graphical dependence spring angles – group of springs

3.4 X-ray diffraction – specimens B

The results of the residual stress measurement are in good line with the results of the winding angles measurements, see chapter 3.3.

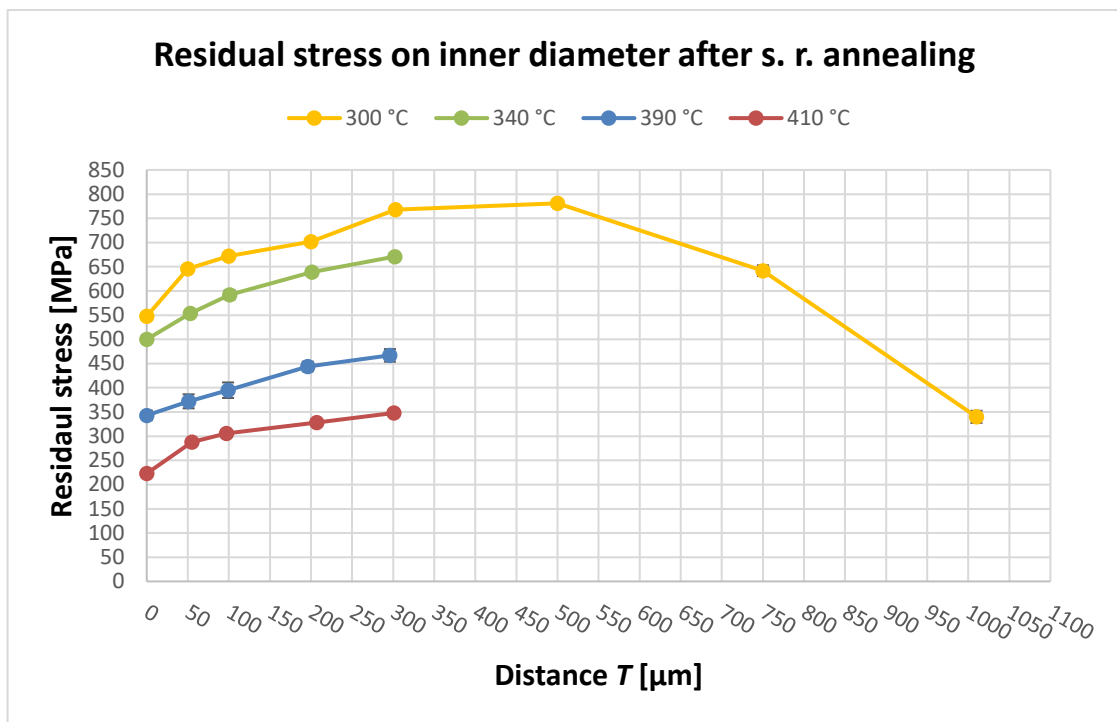


Figure 38: Graphical dependence RS – depth

From Figure 38 it can be concluded that with increasing depth the residual stresses initially increase, which is observable at all temperatures. Lower residual stress values obtained on the surface compared to higher values below the surface could be attributed to cracking when the tensile strength is exceeded. At a temperature of 300 °C the maximum value occurs at a certain point and after that point the residual stress drops. The drop in residual stresses from the maximum value appears to be the result of the equilibrium between the deformed layers and the elastically stretched material layer. Given the theory, for other heat treatment temperatures, a similar course is assumed, with the residual stresses reaching a zero value at a certain depth and gradually becoming the opposite character [3], [32], [33].

3.5 Durability tests – specimens B

The durability test results for the monitored states are shown in Figure 39. It can be seen from the figure that the durability of the springs after annealing at 300 - 390 °C does not much differ. Conversely, the durability of 410 °C annealed state reaches ¼ value compared to other states. With reference to the results of the tensile test (Figure 33), it can be stated that the dependence of the spring durability on the annealing temperature corresponds to the dependence of the strength characteristics on the annealing parameters.

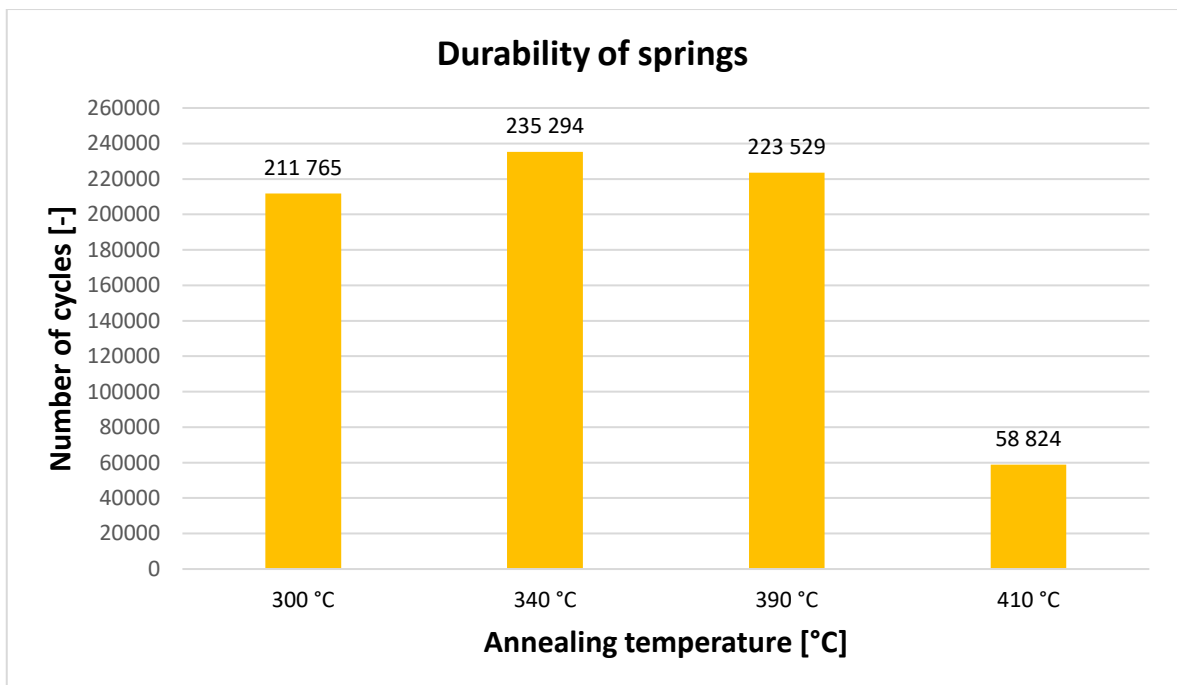


Figure 39: Durability of springs

3.6 General assessment of the HT effect – 4.25 mm wire

Table 15 was compiled for a general assessment of the effect of heat treatment on 54SiCr6 steel properties. It shows selected characteristics, which are evaluated in the form of points. Best equals 4 points, with the maximum $R_{p0.2}$, highest winding angle stability, minimum residual stresses and maximum durability of the compared states being rated as the best in terms of spring properties. For the final evaluation, the sum of the points is decisive, where the best of the compared heat treatments can be considered the one with the most points.

Table 15: General assessment of the HT effect – 4.25 mm wire

Characteristics / furnace temp.	$R_{p0.2}$	Angle stability	Residual stress	Durability	Sum	Overall rating
300 °C	2	4	1	2	9	3.
340 °C	4	3	2	4	13	1.
390 °C	3*	2	3	3	11	2.
410 °C	1**	1	4	1	7	4.

* 380 °C

** 420 °C

From Table 15 it could be concluded that the essential parameter for spring durability is the yield strength $R_{p0.2}$. There is an influence, but less, of the residual stress at the selected heat treatment temperatures.

The most suitable set temperature appears to be 340 °C.

Conclusion

The aim of the submitted thesis was to evaluate the properties and structure of spring steel 54SiCr6 for various conditions of heat treatment. It can be stated:

- 1) Heat treatment - stress relief annealing temperature at selected parameters affects the mechanical properties of the material.
- 2) At annealing temperatures of 300 to 380 °C was not a significant effect of the annealing time in the range of 20 – 40 minutes on properties of the monitored states. However, this effect is significant at a temperature of 420 °C.
- 3) The choice of annealing parameters influences to a lesser extent the steel structure.
- 4) The choice of wire supplier, i.e. the method of spring wire production, affects the mechanical properties and the steel structure after stress relief annealing.
- 5) Temperature of 420 °C should be avoided due to tempering as the strength characteristics are reduced.
- 6) From the point of view of $R_{p0.2}$, winding angle stability, residual stresses and durability within a spring of 4.25 mm wire, the heat treatment temperature of 340 °C seems to be the most suitable.
- 7) The essential parameter for spring durability within a spring of 4.25 mm wire appear to be $R_{p0.2}$. There is also a significant influence of the residual stresses.
- 8) The residual stresses are lower as the annealing temperature rises.
- 9) The results of the residual stress measurement are in good line with the results of the winding angles measurements.
- 10) The choice of annealing temperature affects the winding angle stability and accuracy of spring production, so that with increasing temperature these characteristics decrease.
- 11) The work should be further extended by testing on springs made of both wire diameters from one supplier.
- 12) The work should be also extended by vibration tests on springs at various vibration parameters.
- 13) The work should be further complemented by the influence of $R_{p0.2}$, winding angle stability, durability and residual stresses within a spring of 6.8 mm wire.

The objectives of the thesis were met.

Bibliography

- [1] T. Bauschke, Entstehung der Windeeeigenstressungen und deren Einfluss auf die Ermüdungslebensdauer bei kalt- und halbwarm geformten Fahrzeugfedern, Siegen: Universität Siegen, 2011.
- [2] L. M. Leiseder, Federelemente aus Stahl f für die Automobilindustrie, Landsberg/Lech: Verlag Moderne Industrie, 1997.
- [3] M. Meissner and H.-J. Schorcht, Metallfedern: Grundlagen, Werkstoffe, Berechnung, Gestaltung und Rechnerinsatz, Heidelberg: Springer Verlag, 2015.
- [4] A. Barani, Optimierung der Grenzwerte von Begleitelementen durch innovative Behandlung SiCr-legierter hochfester Stähle für Schraubenfedern, Köln und Hagen: AiF und FSV, 2005.
- [5] "The Bronze Age: Inventions, Tools & Technology," [Online]. Available: <https://study.com/academy/lesson/the-bronze-age-inventions-tools-technology.html>. [Accessed 24 duben 2019].
- [6] D. M. Albert, Are We There Yet?, New York: W. W. Norton & Company, 2019.
- [7] M. Tyndall, "The Past, Present, and Future of Springs," 16 Prosinec 2015. [Online]. Available: <https://www.machinedesign.com/cad/past-present-and-future-springs>. [Accessed 16 Duben 2019].
- [8] S. Copley, "New flexible wishbone could revolutionise vehicle suspension," 6 September 2017. [Online]. Available: <https://www.autocar.co.uk/car-news/industry/new-flexible-wishbone-could-revolutionise-vehicle-suspension>. [Accessed 24 April 2019].
- [9] J. Leinveber and P. Vávra, Strojnické tabulky: učebnice pro školy technického zaměření. Šesté vydání, Úvaly: Albra, 2017.
- [10] A. Bolek and J. Kochman, Části strojů. 5. přeprac, Praha: SNTL - Nakladatelství technické literatury, 1990.
- [11] "Grewis," [Online]. Available: <http://www.grewis.cz/pruziny/talirove-pruziny.php>. [Accessed 29 Duben 2019].
- [12] P. Skočovský, P. Palček, R. Konečná and L. Várkony, Konštrukčné materiály, Žilina: Vydavateľství ŽU, 2000.

- [13] L. Ptáček, *Nauka o materiálu II.*, Brno: CERM, 1999.
- [14] K. Macek and P. Zuna, *Strojírenské materiály*, Vydavatelství ČVUT, 2003.
- [15] H. W. Pollack, *Materials Science and Metallurgy*, 4. edition, New Jersey: Pearson, 1988.
- [16] "Phase Diagrams," 2004. [Online]. Available: <http://www.virginia.edu/bohr/mse209/chapter9.htm>. [Accessed 11 Duben 2019].
- [17] "EO heavy industry," [Online]. Available: <http://www.eoindustry.com/smelting-equipment/steel-smelting-equipment/electric-arc-furnace.html>. [Accessed 6 May 2019].
- [18] "Třinecké železářny," [Online]. Available: <https://www.trz.cz/vyrobky/19/polotovary>. [Accessed 6 May 2019].
- [19] V. Machek, *Kovové materiály 2: vlastnosti a zkoušení kovových materiálů*, Praha: České vysoké učení technické, 2014.
- [20] V. Y. Zubov, "Patenting of steel wire," *Material Science and Heat Treatment*, pp. Volume14, Issue 9, pp 793-800, September 1972.
- [21] K. Macek, P. Zuna and J. Janovec, *Tepelné zpracování kovových materiálů*, Praha: České vysoké učení technické, 2008.
- [22] S. Jayanti, "Hardenability of Steel: Measurement and Factors," [Online]. Available: <http://www.engineeringenotes.com/metallurgy/steel/hardenability-of-steel-measurement-and-factors-metallurgy/26542>. [Accessed 2 August 2019].
- [23] K. Macek, *Kovové materiály*, Praha: Nakladatelství ČVUT, 2006.
- [24] "Hardenability of Steels," 2017. [Online]. Available: <http://www.steeldata.info/hard/demo/data/320.html>. [Accessed 2 August 2019].
- [25] "Material specification sheet: Saarlust - 54SiCr6," Saarlust, [Online]. Available: <https://www.saarlust.com/sag/downloads/download/11543>. [Accessed 2 August 2019].
- [26] G. D. Park and V. L. Tran, "Electrically assisted stress relief annealing of automotive springs," *Journal of Mechanical Science and technology*, 19 April 2017.

- [27] M. A. Yar, Y. Wang and X. Zhou, "Corrosion behaviour of an industrial shot-peened and coated automotive spring steel AISI 9254," *The International Journal of Corrosion Processes and Corrosion Control*, pp. 1-2, 2018.
- [28] A. Silbernagel, A. j. Silbernagel and M. Greger, *Zuštečtování součástí z ocelí českých značek*, Ostrava: Kovosil, 2006.
- [29] J. F. Shackelford, *Introduction to Materials Science for Engineers* (6th edition), New Jersey: Pearson Prentice Hall, 2005.
- [30] "Olin College of Engineering," [Online]. Available: <http://faculty.olin.edu/~jstolk/matsci/Operating%20Instructions/Instron%20Universal%20Tester%20Operating%20Instructions.pdf>. [Accessed 14 August 2019].
- [31] "Oddělení povrchového inženýrství; Katedra materiálu a strojírenské metalurgie; Fakulta strojní; ZČU v Plzni," [Online]. Available: https://www.opi.zcu.cz/Zkousky_tvrdosti.pdf. [Accessed 5 September 2019].
- [32] A. M. Venter, V. Luzin and D. G. Hattingh, "Residual Stresses Associated with the Production of Coiled Automotive Springs," Trans Tech Publications, 2014.
- [33] I. Kraus and N. Ganey, *Difrakční analýza mechanických napětí*, Praha: České vysoké učení technické, 1995.
- [34] I. Kraus and N. Ganey, *Technické aplikace difrakční analýzy*, Praha: Vydavatelství ČVUT, 2004.
- [35] R. N. Penha, L. C. Canale, J. Vatauvuk and S. Lampman, "Tempering of steel," in *Steel Heat Treating - Fundamentals and Processes - Vol. 4A*, Russell Township, ASM International, 2013, pp. 327-351.
- [36] F. Tariq and N. Naz, "Evolution of microstructure and mechanical properties during quenching and tempering of ultrahigh strength low alloy steels," Springer, 2010.
- [37] N. T. Tikhontseva, O. A. Sofrygina and I. Y. Pyshmintsev, "Reversible Tempering Brittleness of Structural," Allerton Press, 2012.

List of figures

Figure 1: Dress pins from the Bronze Age (simple - 1 and threaded - 2) [5]	12
Figure 2: Rifle spring in Radschloss by L. da V. and a modern axle spring [2].....	13
Figure 3: LIFT suspension system by Ariel [8]	15
Figure 4: Ring springs [11]	16
Figure 5: Phase diagram Fe-Fe ₃ C [16]	22
Figure 6: Electric arc furnace [17].....	23
Figure 7: Steel billets [18]	24
Figure 8: Patenting of unalloyed eutectoid steel in the TTT diagram (IT) [19]	25
Figure 9: Relationship between C content, hardness and the amount of martensite [22] .	27
Figure 10: Hardenability diagram of 54SiCr6 steel [24].....	27
Figure 11: Chromium steels and their hardness [21]	28
Figure 12: Spring winding machine Wafios FMU 6.7	30
Figure 13: Continuous gas dual-zone furnace Ipsen.....	31
Figure 14: Stress relief annealing types comparison (t-T) [26].....	33
Figure 15: Stress relief annealing types comparison – t-Residual stress [26]	34
Figure 16: Spring dimensions	38
Figure 17: Laboratory furnace LAC	41
Figure 18: Progress of the heat treatment (t-T dependence of the whole experiment)	42
Figure 19: Specimen after testing.....	43
Figure 20: Mubea simple fixture (made using 3D printing).....	45
Figure 21: Graphical area of PS (Plasticity stock) [19].....	46
Figure 22: EMCO Concept Mill 55 and specimen fixture	47
Figure 23: Leco MSX-255; special clamps; Leco PR4X.....	50
Figure 24: Leco GPX300 - samples polishing.....	50
Figure 25: Angle measuring device	51
Figure 26: Elastic deformation	54
Figure 27: Elastic and plastic deformation (a - load, b - suspension)	54
Figure 28: Difference between load and suspension	54
Figure 29: Re-loading.....	54
Figure 30: The spot of analysing residual stresses.....	56
Figure 31: Overview of specimens, tests and measurements.....	58
Figure 32: Graphical dependence R – ϵ	61
Figure 33: Graphical dependence R _m , R _{p0.2} , HV1 – heat treatment	64
Figure 34: Graphical dependence A _{100 mm} , Z – heat treatment	66
Figure 35: Graphical dependence PS, W – heat treatment.....	68
Figure 36: Metallographic images of specimens A	70
Figure 37: Graphical dependence spring angles – group of springs	71
Figure 38: Graphical dependence RS – depth.....	72
Figure 39: Durability of springs.....	73

List of tables

Table 1: Steel springs and distribution of acting forces and their stresses [2], [10]	17
Table 2: Spring steel representatives [12], [13].....	20
Table 3: Chemical composition and mechanical properties of 54SiCr6.....	35
Table 4: heat treatment parameters of 54SiCr6.....	36
Table 5: Chemical composition and mechanical properties of 54SiCr6 specimens A	37
Table 6: Wire specimens A.....	37
Table 7: Specimens B: springs.....	39
Table 8: Test plan and test marking of specimens A	40
Table 9: Test plan of selected specimens A	49
Table 10: Heat treatment plan for specimens B.....	51
Table 11: Vibration parameters with the number of specimens.....	52
Table 12: Specimens for X-ray diffraction.....	55
Table 13: Test parameters	56
Table 14: Specimens for durability test.....	57
Table 15: General assessment of the HT effect – 4.25 mm wire.....	74